



This is to certify that the

thesis entitled

THE EFFECT OF POLYACRYLAMIDE ON THE PERFORMANCE OF A HYDROCYCLONE

presented by

Lawrence Blair Wallace

has been accepted towards fulfillment of the requirements for

M.S. degree in Chemical Engineering

Major professor

Date_May 5, 1980

O-7639



OVERDUE FINES:

25¢ per day per item
RETURNING LIBRARY MATERIALS:

Place in book return to remove charge from circulation records

THE EFFECT OF POLYACRYLAMIDE ON THE PERFORMANCE OF A HYDROCYCLONE

Ву

Lawrence Blair Wallace

A THESIS

Submitted to
Michigan State University
in partial fulfillment of the requirements
for the degree of

MASTER OF SCIENCE

Department of Chemical Engineering

1980

ABSTRACT

THE EFFECT OF POLYACRYLAMIDE ON THE PERFORMANCE OF A HYDROCYCLONE

Ву

Lawrence Blair Wallace

The centrifugal efficiency of a conical hydrocyclone may be influenced by several distinct flow structures such as turbulent "bursting" phenomena in boundary layers, swirling flow in the central core, and converging flow toward the apex and vortex finder. Because some high molecular weight polymers can affect these flow structures significantly, this study was initiated to determine if the centrifugal efficiency of a hydrocyclone would also be affected by drag reducing polymers. Data reported here show that small amounts of polyacrylamide can either increase or decrease the centrifugal efficiency of a 10 mm hydrocyclone depending on the history of the polymer solution prior to introducing Kaolinite particles. For "pre-stretched" polymers, increases in E greater than 30 percent have been observed for $Re_i > 25,000$. A simplified mathematical model based on a cylindrical hydrocyclone is also developed here. The model is able to make a priori predictions of the performance of a hydrocyclone which agree qualitatively with data obtained from actual hydrocyclones.

Dedicated to

James B. Wallace

ACKNOWLEDGMENTS

The author gratefully acknowledges the guidance and editorial assistance of Dr. Charles Petty.

Funds for this research were provided by the Division of Engineering Research, Michigan State University. This assistance is gratefully appreciated.

Special appreciation is also expressed to my wife, Betty, for her encouragement and help in the completion of this thesis.

TABLE OF CONTENTS

	P	age
LIST	OF TABLES	νi
LIST	OF FIGURES	vii
LIST	OF NOTATION	iх
	PART I AN EXPERIMENTAL STUDY OF THE EFFECT OF POLYMER ADDITIVES ON HYDROCYCLONE PERFORMANCE	
I-1	INTRODUCTION	2
	The Hydrocyclone	2 7
	Structures	8 9 11 11
I-2	DESCRIPTION OF EXPERIMENTAL APPARATUS AND PROCEDURE	13
	Experimental Apparatus	13 13
I-3	DISCUSSION OF RESULTS AND CONCLUSIONS	20
	Drag Reduction Experiments	20
	10 mm Hydrocyclone	23
	Efficiency of a 10 mm Hydrocyclone	31
I-4	RECOMMENDATIONS FOR FURTHER RESEARCH	36

	Page
PART II THEORETICAL PREDICTION OF THE SEPARATIONAL EFFICIENCY OF A CYLINDRICAL HYDROCYCLONE	
II-1 INTRODUCTION	. 39
Motivation	. 39
the Literature	
II-2 FORMULATION OF THE MODEL	. 44
Fluid Mechanics in a Cylindrical Hydrocyclone Particulate Mechanics	. 51
II-3 DISCUSSION OF RESULTS AND CONCLUSIONS	. 59
Computer Program	
Efficiency of a Cylindrical Hydrocyclone	. 62
Case Study II: The Effect of n _V on the Centrifuga Efficiency of a Cylindrical Hydrocyclone Case Study III: The Effect of G on the Cen- trifugal Efficiency of a Cylindrical	. 64
Hydrocyclone	. 68
Research	. 68
APPENDIX A: Experimental Data on Drag Reduction in Pipe Flow	. 71
APPENDIX B: Experimental Data on Solid Liquid Separations in a 10mm Hydrocyclone	. 75
APPENDIX C: Computer Program	. 81
REFERENCES	. 83

LIST OF TABLES

Table		Page
1	The Value of Parameters χ and y for Experiments	28
2	Parameters Specified for Model Studies	60

LIST OF FIGURES

Figure		Page
1	Approximate Dimensions of a 10mm Hydrocyclone	3
2	Important Features of the Flow Structure in a Hydrocyclone	5
3	Particle Size Distribution of Kaolinites	12
4	Experimental Flow Loop	14
5	Flow Through A Manifold of Six 10mm Hydrocyclones	15
6	Chemical Structure of Separan AP-30	18
7	Results of Drag Reduction Experiments Plotted on Prandtl-Karman Coordinates	21
8	The Effect of Separan AP-30 on the Throughput of Six 10mm Hydrocyclones (2 wt.% clay; particle size, 0.77 microns)	25
9	The Effect of Separan AP-30 on the Throughput of Six 10mm Hydrocyclones (2 wt.% clay; particle size, 10.6 microns)	26
10	The Effect of Separan AP-30 on the Flow Ratio (2 wt.% clay; particle size, 0.77 microns)	29
11	The Effect of Separan AP-30 on the Flow Ratio (2 wt.% clay; particle size, 10.6 microns)	30
12	The Effect of Separan AP-30 on the Centrifugal Efficiency of a 10mm Hydrocyclone (2 wt.% clay; particle size, 0.77 microns; polymer concentration, 250 wppm)	32
13	The Effect of Separan AP-30 on the Centrifugal Efficiency of a 10mm Hydrocyclone (2 wt.% clay; particle size, 0.77 microns; polymer concentration, 500 wppm)	33

Figure		Pa	ge
14	The Effect of Separan AP-30 on the Centrifugal Efficiency of a 10mm Hydrocyclone (2 wt.% clay; particle size, 10.6 microns; polymer concentration, 250 wppm)	•	34
15	Path of a Particle of Size 'a' in a Conical Hydrocyclone	•	42
16	Parameters Used to Describe the Performance of a Cylindrical Hydrocyclone	•	45
17	Coordinate System and Path of a Particle of Size 'a' in a Cylindrical Hydrocyclone		54
18	Block Diagram of Computer Program	•	61
19	The Effect of Increasing N on the Centrifugal Efficiency of a Cylindrical Hydrocyclone		63
20	The Effect of Increasing η_{V} on the Centrifugal Efficiency of a Cylindrical Hydrocyclone	•	6 5
21	The Effect of n_v on $n_v J_1(\beta_1 n_v)$ for $\beta_1 = 3.83$	•	6 6
22	The Effect of Increasing G on the Centrifugal Efficiency of a Cylindrical Hydrocyclone		69

LIST OF NOTATION

A = constant relating u_A and r in Eq. (2-4) of Part II

a = radius of an arbitrary particle

D = diameter

d₅₀ = diameter of a particle that gives a centrifugal efficiency
 of 50 percent

E = centrifugal efficiency

f = Fanning's friction factor

f_p = dimensionless pressure drop factor defined in Eq. (3-7) of
 Part I

F_c = centrifugal force acting on a particle in a hydrocyclone

 F_d = drag force acting on a particle in a hydrocyclone

 $G = L/R_{C} = dimensionless variable used in mathematical model$

K = coefficient used to relate α and Re; in Eq. (3-8) of Part I

L = length of hydrocyclone; length of tube used in drag reduction experiments

N = defined in Eq. (2-41c) of Part II

n = exponent relating u_{θ} and r in Eq. (3-6) of Part I

 ΔP = pressure drop

 ΔP^* = pressure drop across the hydrocyclone excluding losses due to to entrance effects

Q = volumetric flow rate through the hydrocyclone

Re = Reynolds number

 $R_f = w_u/w_r = flow ratio$

T = temperature

- u = velocity
- u_h = bulk average velocity
- W_f = feed mass flow rate
- w., = underflow mass flow rate
- \underline{w} = vorticity
- y = exponent used to relate α and Re; in Eq. (3-8) of Part I

Greek Letters

- α = velocity reduction factor
- β_{0} = first zero of J_{0} (·)
- β_1 = first zero of J_1 (·)
- η = r/R_c = dimensionless variable used in mathematical model
- λ = constant introduced in solution of Eq. (2-23) of Part II
- μ = viscosity
- ξ = z/L = dimensionless variable used in mathematical model
- ρ = density
- ρ_s = density of particle
- χ = parameter defined in Eq. (3-10) of Part I
- ψ = stream function

<u>Subscripts</u>

- e = on the equilibrium line of a particle in the hydrocyclone
- N = at the entry point of the critical particle into the centrifugal force field
- p = pertaining to the particle

- pr = radial component of particle
- pz = vertical component of particle
- r = radial component in cylindrical coordinate system
- θ = tangential component in cylindrical coordinate system
- z = vertical component in cylindrical coordinate system

PART I

AN EXPERIMENTAL STUDY OF THE EFFECT OF POLYMER ADDITIVES ON HYDROCYCLONE PERFORMANCE

I-1. INTRODUCTION

The Hydrocyclone

The cyclone is a device that uses a centrifugal force field induced by the rotational motion of a fluid to separate materials having different properties. When a cyclone is designed specifically for liquids it is referred to as a hydrocyclone (see Bradley, 1965). Figure 1 is a schematic of a typical hydrocyclone. The upper cylindrical portion contains the tangential feed inlet and a cylindrical outlet tube located axially. The outlet tube is commonly referred to as the overflow pipe or as the vortex finder. The lower conical portion of the hydrocyclone contains a circular opening at its apex called the underflow orifice. The dimensions given in Figure 1 are those of the hydrocyclone used in this study.

Fluid containing the material to be separated enters the hydrocyclone through the tangential inlet. The cylindrical geometry causes the fluid to flow in a circular path toward the apex. The fluid in the outer region leaves through the underflow orifice, and the fluid in the inner region reverses its direction and exits through the vortex finder. Solid particles suspended in the fluid will be affected by the centrifugal force field. Some particles will migrate to the outer regions of the hydrocyclone and thus will be concentrated in the fluid leaving through the underflow orifice.

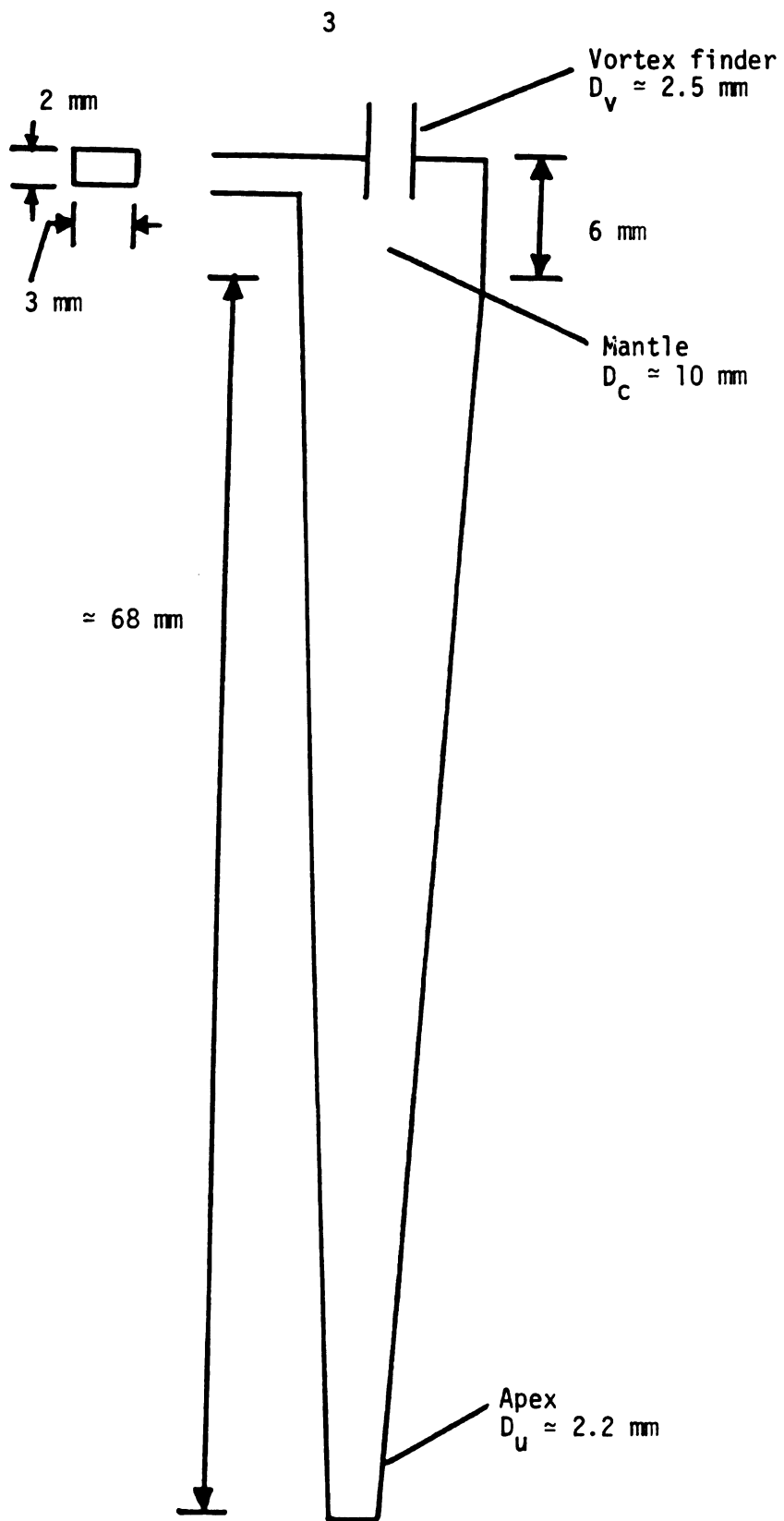


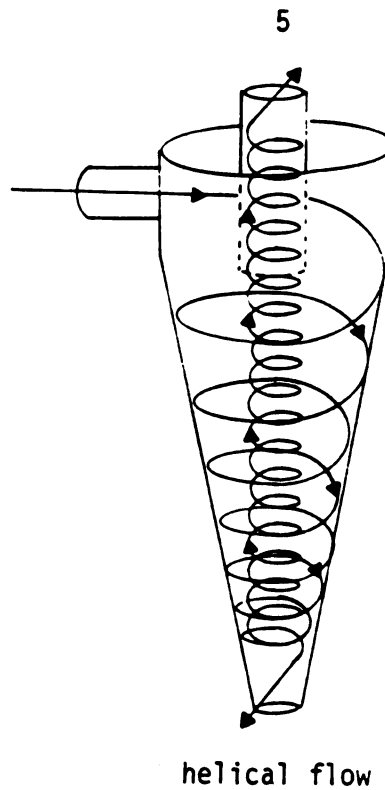
Figure 1.--Approximate Dimensions of a 10 mm Hydrocyclone.

Other particles will migrate toward the inner region of the hydrocyclone and exit with the fluid leaving through the vortex finder.

Figure 2 illustrates qualitatively the main features of the flow pattern in a typical hydrocyclone. The most prominent features are a downward spiral in the outer region and an upward spiral in the inner region. Because the fluid in the outer spiral and the fluid in the inner spiral have vertical velocity components in opposite directions, there must be a surface of zero vertical velocity. Dye studies by Bradley and Pulling (1959) indicate that, in the cylindrical portion, the locus of zero vertical velocity is a cylinder coaxial with the hydrocyclone and having a radius of .43 $\rm D_{\rm C}$. In the conical portion of the hydrocyclone, Kelsall (1952) obtained data that implies that the locus of zero vertical velocity is conical with its apex at the apex of the hydrocyclone.

Rotation of the liquid in the inner spiral forms a low pressure core. This results in the formation of a free liquid surface. If the vortex finder or the underflow orifice is open to the atmosphere, the core becomes filled with air. If neither the vortex finder nor the underflow orifice is open to the atmosphere the core may still exist depending on the back pressure at the underflow orifice and the vortex finder.

A portion of the solid suspension entering through the feed inlet short circuits directly to the overflow. Kelsall (1953) demonstrated that under certain conditions this flow can be as much as 15 percent of the feed. Not all of the fluid in the inner spiral



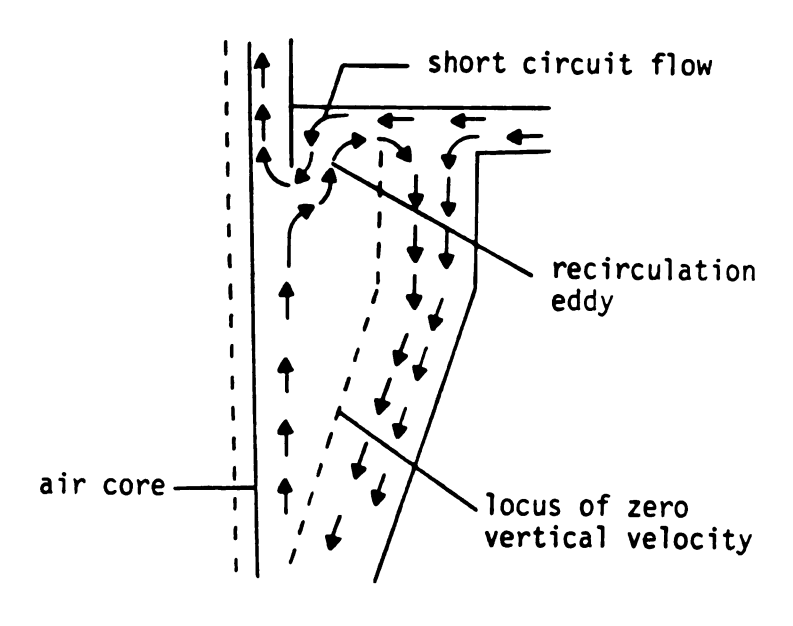


Figure 2.--Important Features of the Flow Structure in a Hydrocyclone.

can exit through the vortex finder. The excess is recirculated forming eddies. Near the hydrocyclone wall, the phenomena associated with boundary layer flow will occur while in the inner regions the flow has characteristics similar to that of a free vortex. Also near the underflow orifice and the vortex finder, convergent velocity fields exist.

Kelsall (1952) used an optical technique to measure the velocity components of water in a 3" diameter hydrocyclone. With an inlet velocity of 14 ft/sec., Kelsall found that the axial velocity near the wall was -5 ft/sec. and near the air core was +20 ft/sec. The radial velocity had a maximum value of 1 ft/sec. inward near the cone wall, and decreased to zero as the air core interface was approached. Kelsall also found outward radial flow in the upper regions of the hydrocyclone where the eddies occur. The tangential velocity was 13 to 17 ft/sec. near the wall of the conical section and increased to a maximum of 50 ft/sec. away from the wall before falling to 27 ft/sec. at the air core interface. The maximum tangential velocity occurred at a radius of 0.18". If Kelsall's data are extrapolated back to the radius of the inlet, it indicates that there is a drop in velocity as the feed enters. This is common to all hydrocyclones with reduction by factors of 0.4 to 0.8 being typical (Bradley, 1965).

The range of values of the centrifugal acceleration in the 3" hydrocyclone can be easily deduced from the values of u_{θ} , and range from 25 to 5,000 times the acceleration of gravity. Because

of the magnitude of the centrifugal acceleration produced in hydrocyclones the effect of gravity is negligible and a hydrocyclone may be operated in a horizontal position as effectively as in a vertical position.

Turbulence in Hydrocyclones

The inlet Reynolds number, defined by

$$Re_{i} = \frac{u_{i}D_{i}^{\rho}}{u}, \qquad (1-1)$$

is 10⁴ to 10⁵ in typical hydrocyclone applications. These values indicate that the flow in the inlet pipe is normally turbulent. Using an electrochemical technique, Rietema (1963) measured the turbulent intensities at various points in a 3" hydrocyclone. The data presented implies that the turbulent intensity varies from 10 percent at the inlet to an average of 2 percent near the outer wall of the cylindrical section. The drop in turbulent intensity was postulated to arise because of the circular motion of the liquid within the hydrocyclone. Reitema's work, while providing insight into the nature of the flow in hydrocyclones, is limited because only one hydrocyclone geometry was studied. It is not clear that these results can be extrapolated to other hydrocyclones.

Flow visualization studies (Kline, et al., 1967; Nychas, et al., 1973) of turbulent flow fields have established the existence of a bursting phenomena in the turbulent boundary layer structure. The effect of turbulent bursting on the efficiency of hydrocyclones is clearly unfavorable. Solid particles near the wall would

normally be carried out of the hydrocyclone through the underflow orifice. The bursting phenomena interferes with this process by scattering the particles from the wall back into the inner region of the hydrocyclone. Depending on the level at which this occurs, the particle might not have enough time to be transported back to the wall by the centrifugal force field before it is carried out of the hydrocyclone in the overflow stream. Because of the potentially large effect of turbulence on efficiency, this aspect of hydrocyclone operation deserves further attention.

The Effect of Dilute Polymer Solutions on Flow Structures

The phenomena of drag reduction by dilute polymer solutions, recently reviewed by Virk (1975) and Berman (1978), was discovered by Toms (1948) and Mysels (1949). They found that a significant reduction in skin friction caused by the turbulent flow of a Newtonian fluid past a solid surface can be achieved by the addition of a small amount of polymeric material to the liquid. The effect of dilute polymer solutions on the bursting phenomena in turbulent boundary layers has been studied by Donohue, et al. (1972). These experiments indicate that the spatially averaged bursting rate is greatly decreased by the addition of the polymer. With a liquid velocity of .207 m/sec., Donohue measured an 80 percent decrease in the bursting rate between water and a 139 wppm polyethylene oxide solution.

Experiments involving vortex inhibition by dilute polymer solutions for non-turbulent rotational flows have been reported by

Chiou and Gordon (1976). The maximum tangential velocity of a vortex was found to decrease from 37 cm/sec. in water to 3 cm/sec. in a 3 wppm Separan AP-273 solution. The formation of an air core was found to be inhibited in solutions with polymer concentrations as low as 1.5 wppm.

Studies on the behavior of non-turbulent, non-rotational converging flows of viscoelastic and Newtonian fluids have been reported by Metzner, et al. (1969). Results indicate that the pressure drop for flow from a large reservoir to a small tube was larger for the dilute polymer solution. The presence of the polymer also induced strong secondary motions near the entry of the small tube. Thus, dilute polymer solutions may have unfavorable as well as beneficial effects on the efficiency of a hydrocyclone. Favorable effects may arise from the suppression of the bursting phenomena, while the decrease in tangential velocities could lead to a decrease in efficiency. The effect on converging flows suggest that larger pressure drops across the hydrocyclone may be necessary for dilute polymer solutions.

Hydrocyclone Efficiency

Efficiency definitions have been developed to allow the comparison of the performance of various types of separational equipment. The definitions are thus not only applicable to hydrocyclones, but to any separational device whose performance does not change with time.

The centrifugal efficiency of a hydrocyclone is defined as the fraction of solids in the feed separated due to the action of the centrifugal force field. Kelsall (1953) assumed that the fraction of solids in the feed entrained by the underflow and not subjected to the centrifugal force field equals the fraction of liquid in the feed that leaves through the underflow. The centrifugal efficiency is then the fraction of the remaining solids in the feed that is separated. This leads to the following definition for the centrifugal efficiency

$$E = \frac{E_{T} - R_{f}}{1 - R_{f}}$$
 (1-2)

where.

E is the centrifugal efficiency

 E_T is the gross efficiency, i.e., the ratio of the mass flow rate of solids in the feed to the mass flow rate of solids in the underflow

 R_{f} is the ratio of underflow to feed volumetric flow rates. R_{f} is an approximation to the ratio of liquid flow rates in the underflow and feed so that equation (1-2) is strictly valid only for dilute solid suspensions. Although the assumptions inherent in the development of equation (1-2) are not rigorously correct, this definition of efficiency does provide a measure of the centrifugal action of the hydrocyclone and, unlike other definitions, satisfies the inequality $0 \le E \le 1$.

Experimental Objectives

The effect of polymer additives on hydrocyclone performance can be inferred by studying the centrifugal efficiency over a range of Reynolds numbers. The Reynolds number, defined by equation (1-1), was varied from 10⁴ to 4 x 10⁴. Two grades of Kaolinite clays, differing in their particle size distribution, were utilized as part of this research. The median particle sizes of the two clays were 0.77 microns and 10.6 microns (see Figure 3). Although .77 microns is smaller than the normal particle size separated effectively by hydrocyclones, it was felt that particles of this size would be more susceptible to the turbulent re-entrainment forces. Thus, the major hypothesis of this research is that the effect of polymer additives on turbulent diffusion can be studied indirectly by examining the centrifugal efficiencies of hydrocyclones operating on the two clays.

Significance of This Research

The advantages of hydrocyclones have led to their widespread use as inertial separators. One aspect of hydrocyclone operations that has restricted its application is the presence of a lower limit on the particle size which can effectively be separated (Bradley, 1965); therefore, discovery of an increase in the efficiency of hydrocyclones operating on very small particles due to polymer additives may lead to new areas of application.

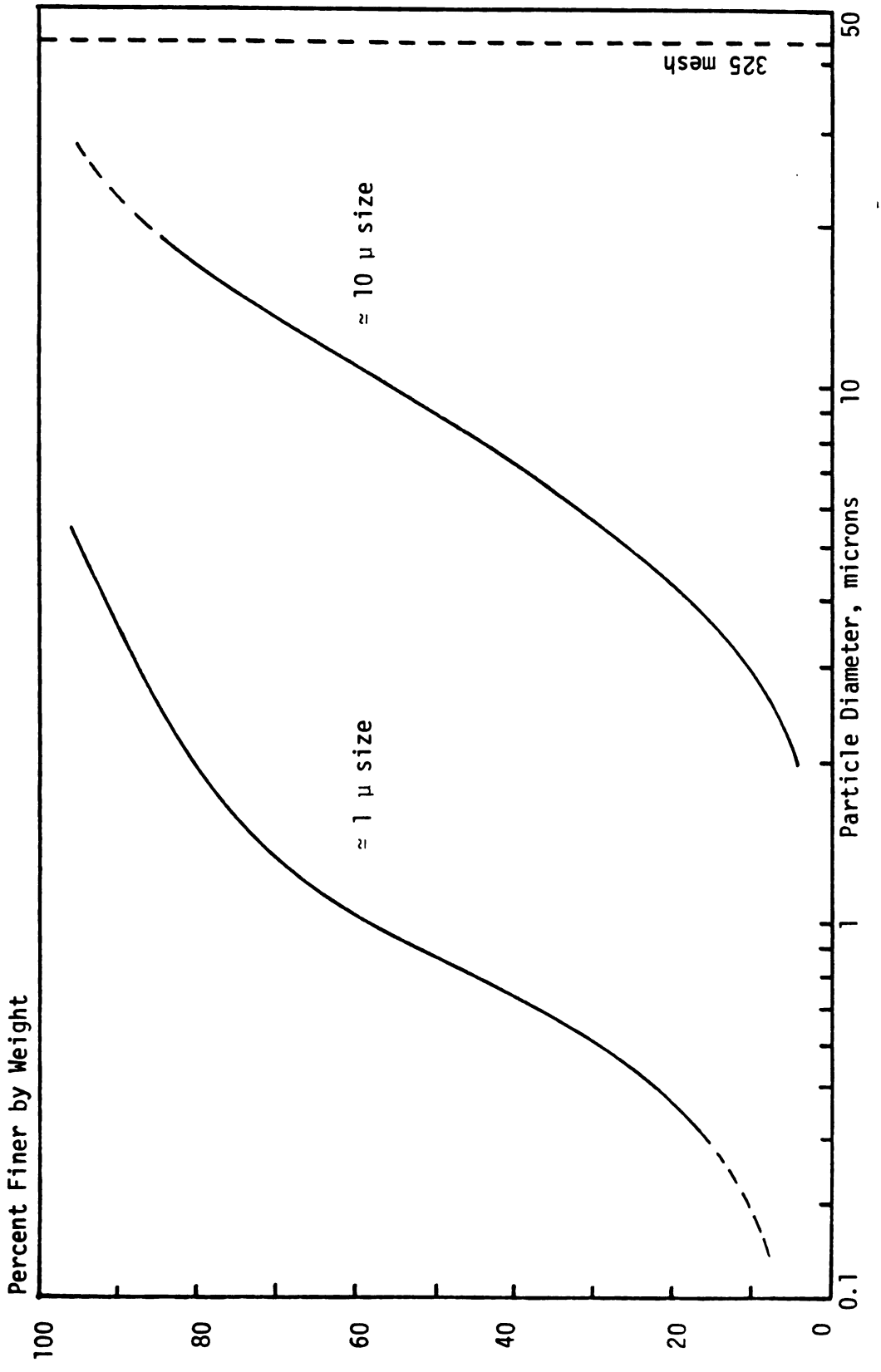


Figure 3.--Particle Size Distribution for "olinites (Furnished by Georgia Kaolin Company).

I-2. DESCRIPTION OF EXPERIMENTAL APPARATUS AND PROCEDURE

Experimental Apparatus

A schematic of the flow loop used to carry out the experiments is shown in Figure 4. The hydrocyclone, marketed as an impurity eliminator by Dorr-Oliver, is actually a cluster of six 10 mm hydrocyclones (see Figure 1). The six hydrocyclones operate in parallel and are fed by a common manifold. The path of the fluid through the manifold is shown in Figure 5. The overflow and underflow streams of the hydrocyclone manifold are open to the atmosphere. Two centrifugal pumps (Myers, QP 30-3) connected in series provided a feed flow to the hydrocyclones with pressures up to 100 psi. The loop was designed so that a portion of the flow was recycled from the high pressure side of the pumps back into the reservoir. This gave good control of the flow through the loop and also kept the suspension in the reservoir well agitated. The purpose of the straight pipe located over the reservoir was to carry out drag reduction experiments. The pipe was 3/16" I.D. drawn copper tubing and measured 5' between the pressure taps.

Experimental Procedures

The centrifugal efficiency of the hydrocyclone was determined by measuring the underflow and overflow mass flow rates at a

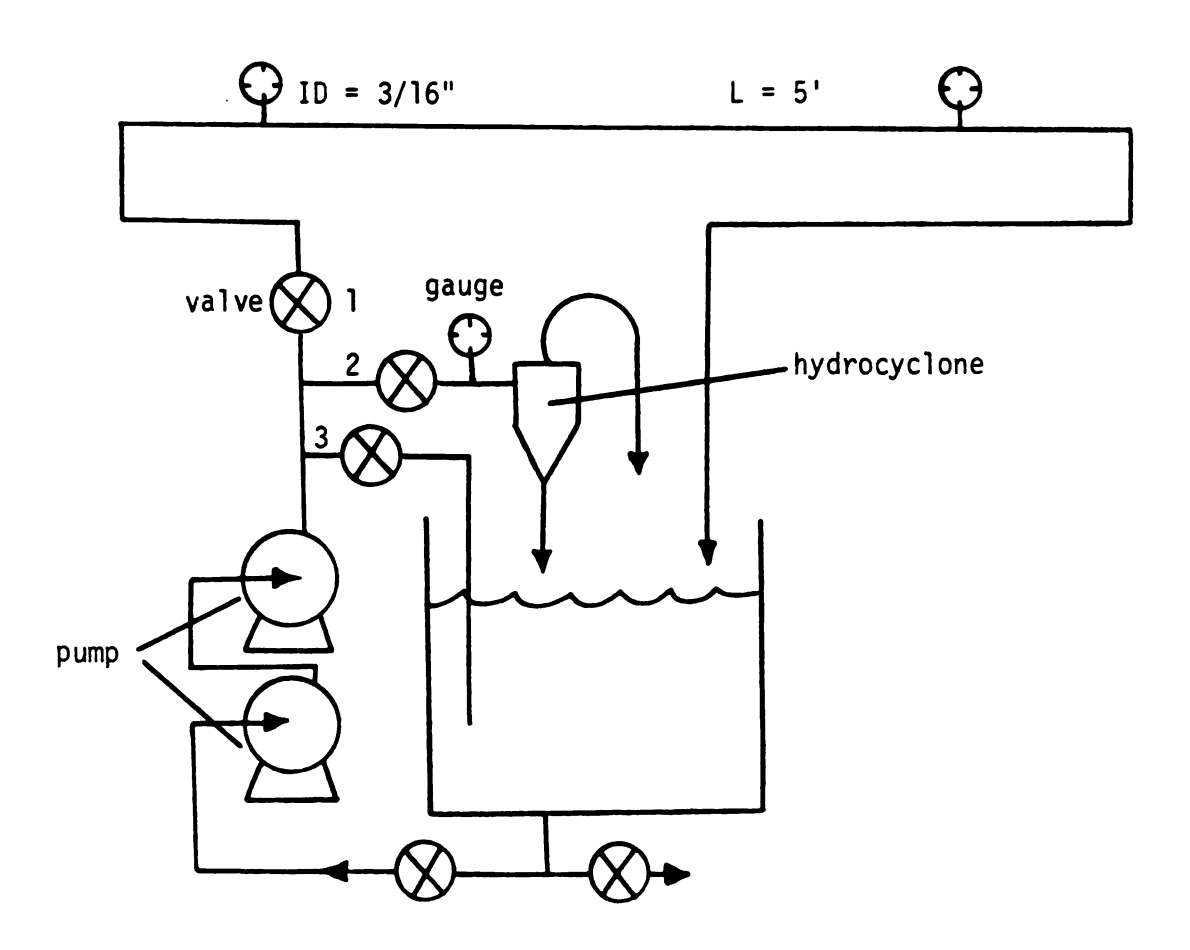


Figure 4.--Experimental Flow Loop.

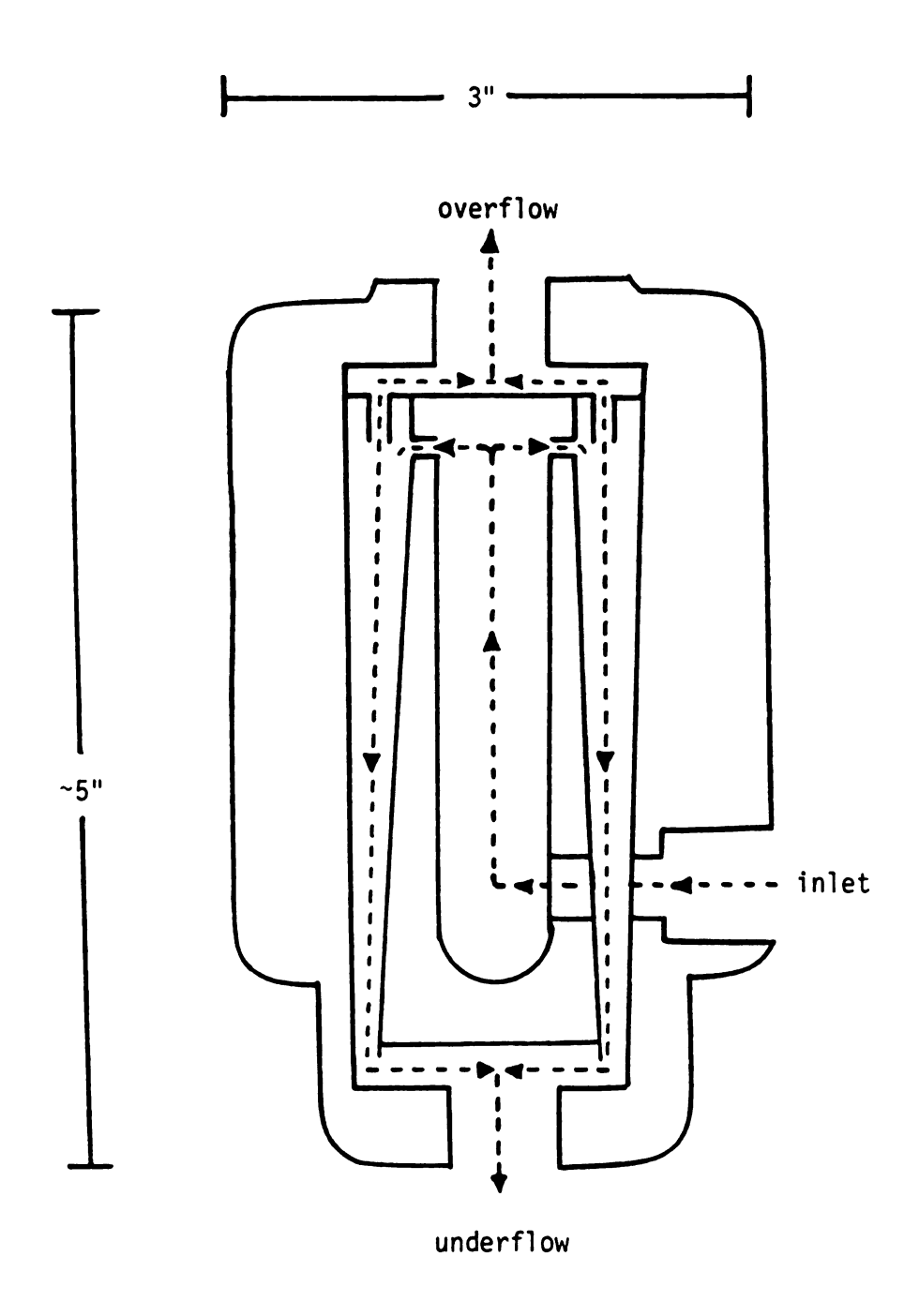


Figure 5.--Flow Through a Manifold of Six 10 mm Hydrocyclones.

number of pressure drops across the hydrocyclone. The mass flow rates were measured directly by weighing a sample collected over a measured time interval. Samples of the underflow, overflow, and the suspension in the reservoir were taken as the mass flow rate data were being obtained. These samples were analyzed gravimetrically to give the concentration of clay particles in each stream entering and leaving the hydrocyclone. Data were collected for pressure drops across the hydrocyclone ranging from 10 psi to 100 psi at 10 psi intervals. The pressure at the inlet was indicated by a standard pressure gauge. Because the underflow and overflow lines were open to the atmosphere, this reading was assumed to represent the pressure loss across the hydrocyclone.

Samples of the overflow, underflow, and reservoir were collected in 8 oz. bottles. At high flow rates, the agitation in the reservoir was decreased because of decreased flow through Valve 3. In order to insure that a well mixed sample of the contents of the reservoir was obtained, the effluents from the overflow and underflow pipes were collected together and the resulting mixture was sampled. The concentration of the solids in these samples was determined by drying a 3 to 4 gram aliquot.

The valves labeled 1, 2, and 3 in Figure 4 were used to control the flow through the loop. During the experiments, Valve 3 was normally left full open and the flow through the loop was controlled by Valves 1 and 2. At high flow rates, Valve 3 was partially closed in order to dampen the fluctuations in flow through the loop.

The drag reduction experiments consisted of simultaneously measuring the pressure drop and the mass flow rate through the straight pipe. The procedure followed was to achieve a constant pressure drop across the pipe by manipulating Valve 1, and then to measure the mass flow rate through the pipe. Three measurements of the mass flow rate were obtained at each pressure drop. The pressure drop was set at intervals of 5 psi from 5 psig to 30 psig. The pumps were operated for approximately 15 minutes to obtain the data over the given pressure drop range. During this time the temperature of the fluid in the loop rose approximately 10° C. The temperature change was closely monitored by measuring the temperature of the fluid each time the mass flow rate was measured.

The polymer used in the experiments was Separan AP-30, manufactured by Dow Chemical Company. This copolymer of polyacrylamide and polyacrylic acid (see Figure 6) has a molecular weight in the range of 860,000 to 1,000,000 (Blanks, et al., 1974). The polymer solution used in the experiments was prepared by dissolving 20 grams of polymer in one gallon of water and mixing this solution with 20 gallons of water in the reservoir. Eight, 2.5 gram portions of the polymer were dissolved in water by mixing each portion with 500 ml of water in a Waring blender for five minutes. The resulting solution was deaerated by placing it under a vacuum in a vacuum flask. When the one gallon polymer solution was diluted in the reservoir the polymer concentration was approximately 251 wppm.

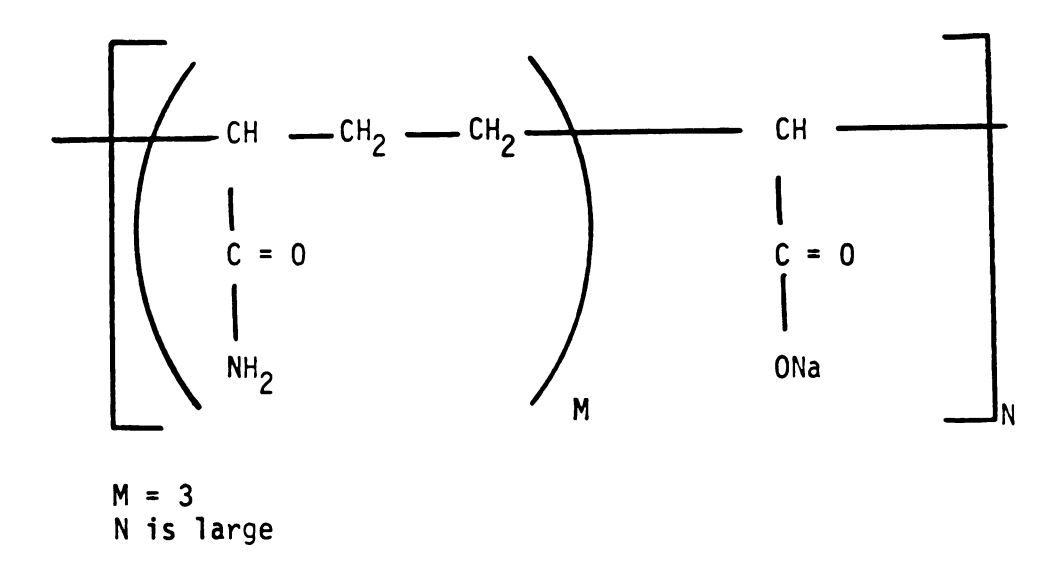


Figure 6.--Chemical Structure of Separan AP-30.

The strategy for preparing the clay-polymer-water suspension is crucial. One method of conducting the experiments was to begin by obtaining pressure drop versus flow rate data for water in the straight pipe. Enough clay was then added to the water in the reservoir to make an approximately 2 wt percent clay suspension. Separation experiments in the hydrocyclone were then carried out using this suspension. After the reservoir had been drained and cleaned, the polymer solution was mixed in the reservoir and pressure drop versus flow rate measurements on the straight pipe were repeated. After adding clay to the polymer solution, separation experiments in the hydrocyclone were repeated. This sequence was followed in all but one series of tests in which the drag reduction experiments were not conducted prior to the separation studies. The results of this series differed significantly from those of the other series and will be discussed in the next chapter.

I-3. DISCUSSION OF RESULTS AND CONCLUSIONS

Drag Reduction Experiments

The purpose of the drag reduction experiments was to show that the polymer solutions used in the hydrocyclone experiments possessed drag reducing properties. The data obtained are given in Appendix A. These data are plotted on Prandtl-Karman coordinates in Figure 7, where

$$f \equiv \frac{g_c (-\Delta P) D}{2 u_b^2 \rho L}, \text{ and}$$
 (3-1)

$$Re \equiv \frac{D u_b \rho}{u} \qquad (3-2)$$

 ΔP is the pressure drop; u_b is the bulk average velocity; D is the diameter of the pipe and L its length; ρ and μ represent, respectively, the density and viscosity of the fluid. The viscosity used in equation (3-2) is calculated by

$$\frac{1}{11} = 2.1482[(T-8.435) + \sqrt{8078.4 + (T-8.435)^2}] - 120$$
 (3-3)

(see p. 778 in Bennett and Myers, 1962) where T is the temperature of the fluid in degrees centigrade.

The ordinate of Figure 7 represents a ratio of bulk to turbulent velocities while the abscissa is a ratio of pipe to

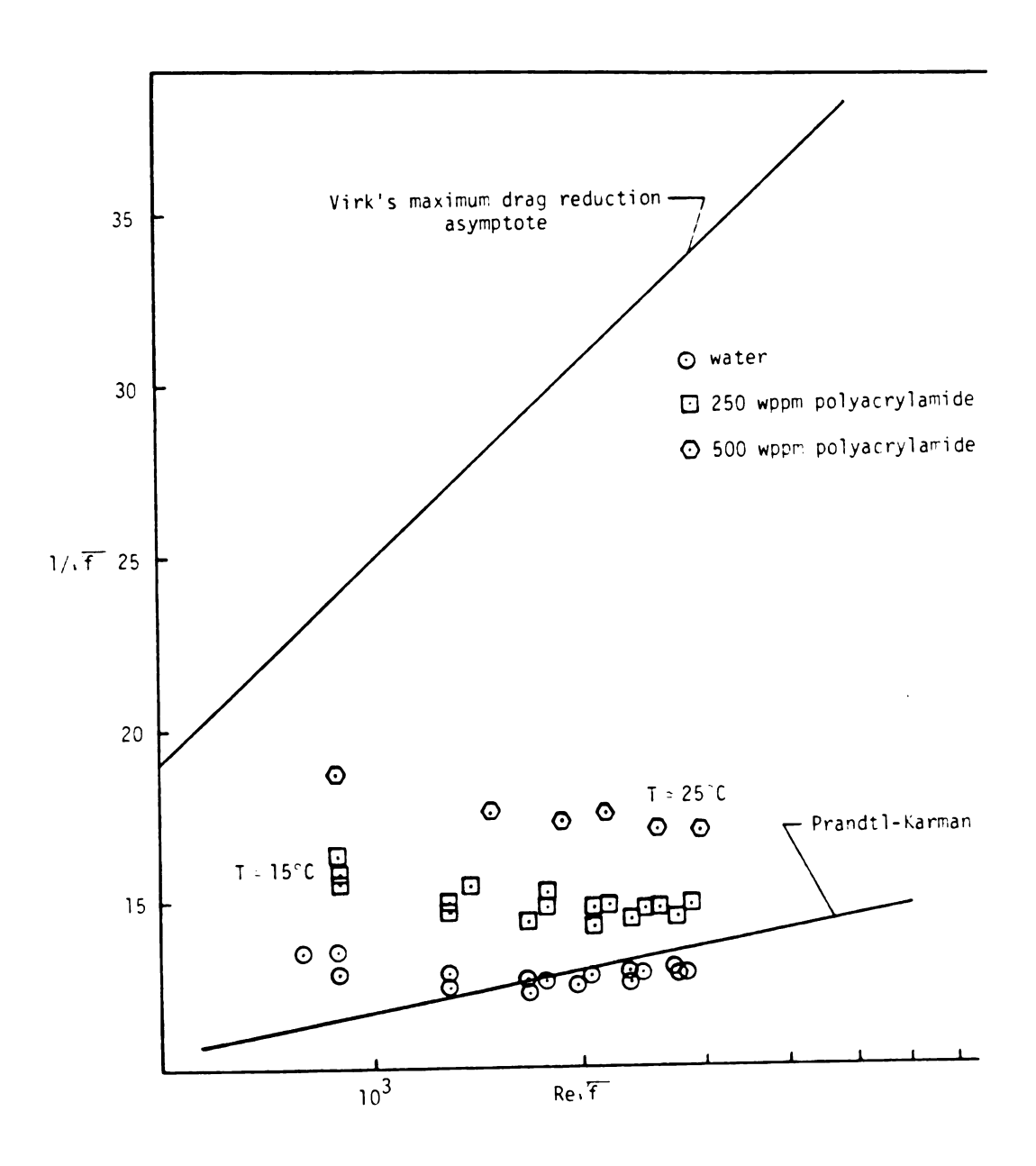


Figure 7.--Results of Drag Reduction Experiments Plotted on Prandtl-Karman Coordinates.

turbulent length scales. Thus, according to Virk (1975), the Prandtl-Karman coordinates are the most natural for correlating drag reduction data in pipes. The lower solid line in Figure 7 represents the Prandtl-Karman law,

$$\frac{1}{\sqrt{f}}$$
 = 4.06 log (Ref²)-0.4 (3-4)

which describes the turbulent flow of Newtonian fluids in smooth pipes. The data for water fall near this line except for the data points below 10^3 on the abscissa. This descrepancy can be explained by examining the precision of the experimental measurements for these points. Because of pressure fluctuations in the apparatus, the pressure drop across the straight pipe could be measured with an accuracy of only \pm 1 psi. This translates into an uncertainty of \pm 2 ordinate units for the initial points in Figure 7. Thus the distance from the Prandtl-Karman law for all of the data for water are less than experimental error.

The upper solid line in Figure 7 represents the maximum drag reduction asymptote described by Virk (1975). This asymptote has been widely observed and is insensitive to polymer species, molecular weight, and concentration. Polymer solutions should fall close to this asymptote for values of the abscissa above 10^3 . The failure of the data for the polymer solutions used in this experiment to approach the maximum drag reduction asymptote may be due to polymer degradation.

Sylvester and Kumor (1973) found that dilute solutions of Separan AP-30 undergoing degradation exhibit three distinct regions in their flow regimes. At the beginning of the degradation studies the polymer solution flow data fell on the maximum drag reduction asymptote. As the polymer was degraded the flow data exhibited a linear increase in the friction factor for a given throughput. As the degradation further increased the friction factor for the polymer solutions approached the Prandtl-Karman law. Figure 7 shows that, while the polymer solutions used in the experiments do have drag reducing properties, they were degraded.

The Effect of Polymer on the Capacity of a 10 mm Hydrocyclone

The experiments were carried out with the objective of determining the effects of a polymer additive (Separan AP-30) on the performance of a 10 mm hydrocyclone. The results of the experiments are given in tabular form in Appendix B and are shown graphically in the following discussion.

Two strategies for preparing the polymer solution were followed. In all of the experiments except for series II, the polymer-water solution was sheared in the 3/16" tube prior to mixing with the clay (mixing strategy I). In series II, this was not done; the hydrocyclone experiments were run immediately after the polymer solution was prepared (mixing strategy II). Thus, the polymer solution made up following mixing strategy II was not subjected to the same intense vortex stretching turbulent structures

characteristic of pipe flow (Kline, et al., 1967 and Nyochas et al., 1973). It is noteworthy that differences in mixing strategy did not change the effect of the polymer solutions on the throughput of the hydrocyclone, as indicated by Figures 8 and 9, but had a pronounced effect on the centrifugal efficiency.

Figures 8 and 9 show that for a given pressure drop, the total flow rate is reduced by the presence of the polymer. At pressure drops between 80 and 100 psi, the flow rate through the hydrocyclone was reduced by approximately 5 percent by the 250 wppm polymer solution and by approximately 8 percent when the polymer concentration was increased to 500 wppm (see tabulated data in Appendix B). The origin of this phenomenon may arise because of different flow structures in the entrance region of the hydrocyclone, as explained below.

By taking a force balance on an element of fluid rotating in the hydrocyclone, Bradley (1965) obtained

$$\frac{dP}{dr} = \frac{\rho u_{\theta}^2}{r}, \qquad (3-5)$$

where P is the pressure, \mathbf{u}_{θ} is the tangential velocity, and r is the radial position in the hydrocyclone. If \mathbf{u}_{θ} and r are related by

$$u_{\theta} r^{n} = constant \equiv \alpha u_{i} \left(\frac{D_{c}}{2}\right)^{n}$$
, (3-6)

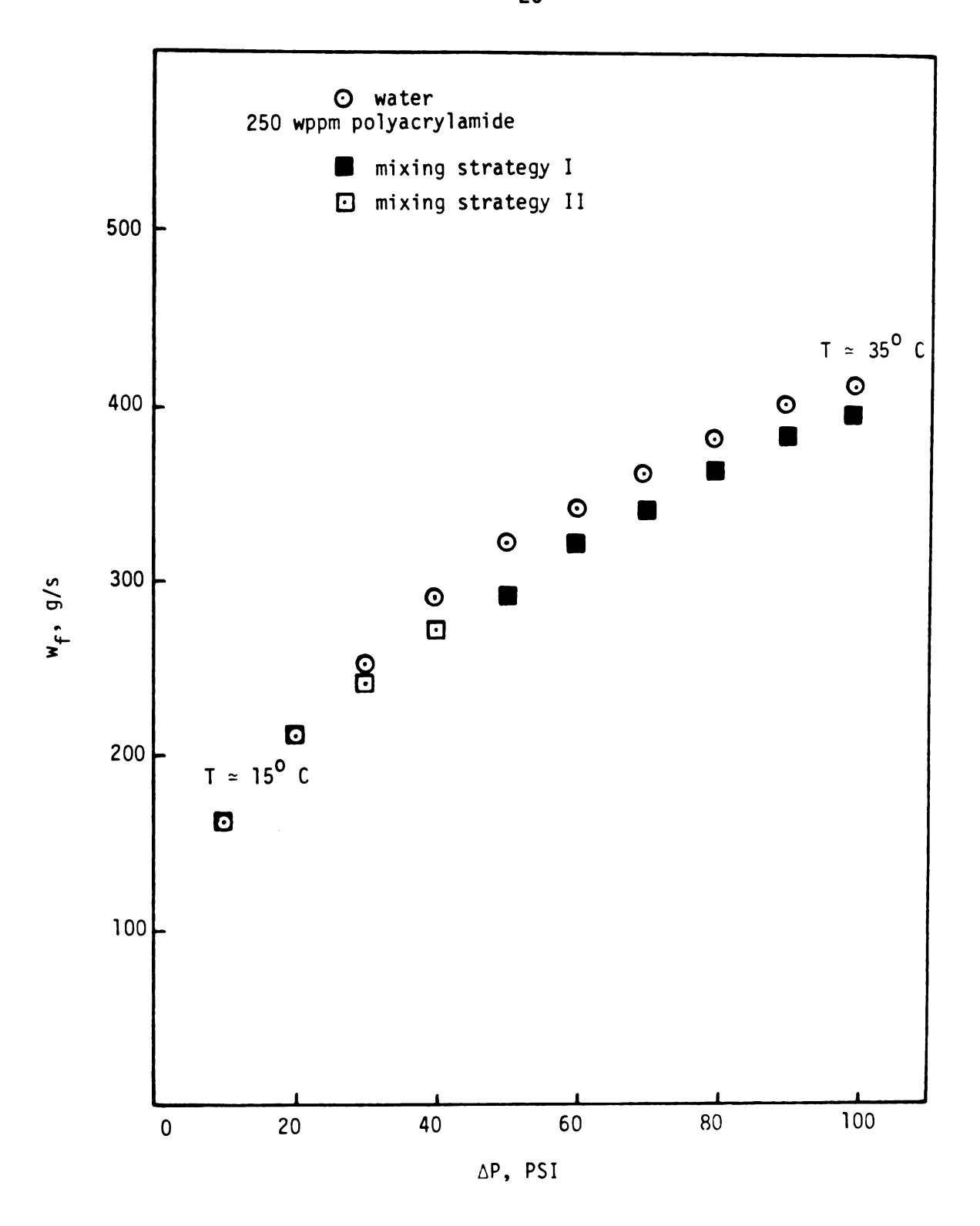


Figure 8.--The Effect of Separan AP-30 on the Throughput of Six 10 mm Hydrocyclones (2 wt% clay; particle size, 0.77 microns).

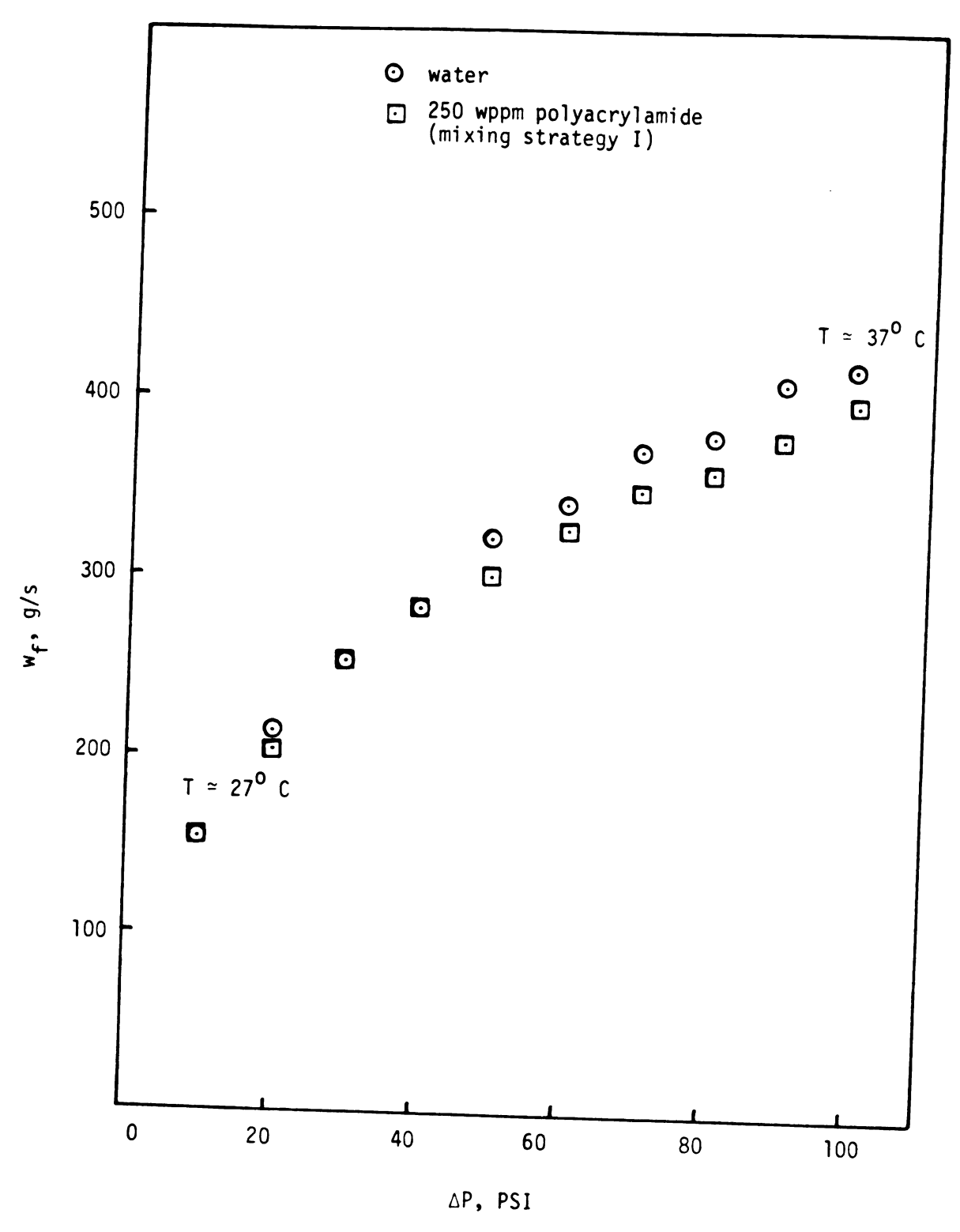


Figure 9.--The Effect of Separan AP-30 on the Throughput of Six 10 mm Hydrocyclones (2 wt% clay; particle size, 10.6 microns).

then integrating equation (3-5) between the radius of the vortex finder and the radius of the hydrocyclone yields

$$f_p = \frac{\Delta P^*}{\frac{1}{2}\rho u_i^2} = \frac{\alpha^2}{n} \left[\left(\frac{D_c}{D_v} \right)^{2n} - 1 \right] .$$
 (3-7)

 ΔP^{\star} does not include pressure losses due to entry effects; however, α accounts for the velocity loss at the inlet.

 α has been found to be dependent on flow rate while n is much less dependent on operating variables (Bradley, 1965). Assuming that the functional relationship between α and the flow rate is

$$\alpha = K \operatorname{Re}_{i}^{y}$$
, (3-8)

where K and y are constants, gives

$$f_p = \chi Re_i^{2y}$$
 , (3-9)

where χ is a parameter given by

$$\chi = \frac{K^2}{n} \left[\left(\frac{D_c}{D_v} \right)^{2n} - 1 \right] . \tag{3-10}$$

Assuming that $\Delta P^* \cong \Delta P$, a least squares analysis of the data for the small particle size clay gives values for χ and y shown in Table 1. Note that the addition of polymer causes the value of χ to decrease and the value of y to increase. Equation (3-10) shows that χ could have been reduced through either a reduction in K or n.

Figures 10 and 11 show the effect of the polymer on the flow ratio $R_{\mathbf{f}}$, i.e., the ratio of the underflow rate to the feed flow rate of the hydrocyclone. The flow ratio decreases with increasing throughout until a minimum at 300 g/s for the total flow rate. At higher values of the throughput the data becomes irregular and the flow ratio tends to increase. Figures 10 and 11 also show that the addition of polymer tends to decrease $R_{\mathbf{f}}$ at a given throughput.

Table 1.--The Value of Parameters χ and y for Experiments.

Parameters	Composition of Fluid Phase		
	Water	250 wppm Polyacrylamide Solution	500 wppm Polyacrylamide Solution
X	. 490	. 374	.326
у	. 165	.184	.193

If the value of n were increased by the addition of polymer, then equation (3-6) predicts that there would be a flattening out of the tangential velocity profile as reported by Chiou and Gordon (1976) for rotational flows in large vessels. This phenomena, if it occurs, could explain the observed decrease in $R_{\mbox{\scriptsize f}}$ with polymer addition, provided the magnitude of the underflow rate is controlled by the effect of $u_{\mbox{\scriptsize θ}}$ on the boundary layer. However, if the underflow rate is determined by the size of the air core and if this decreases

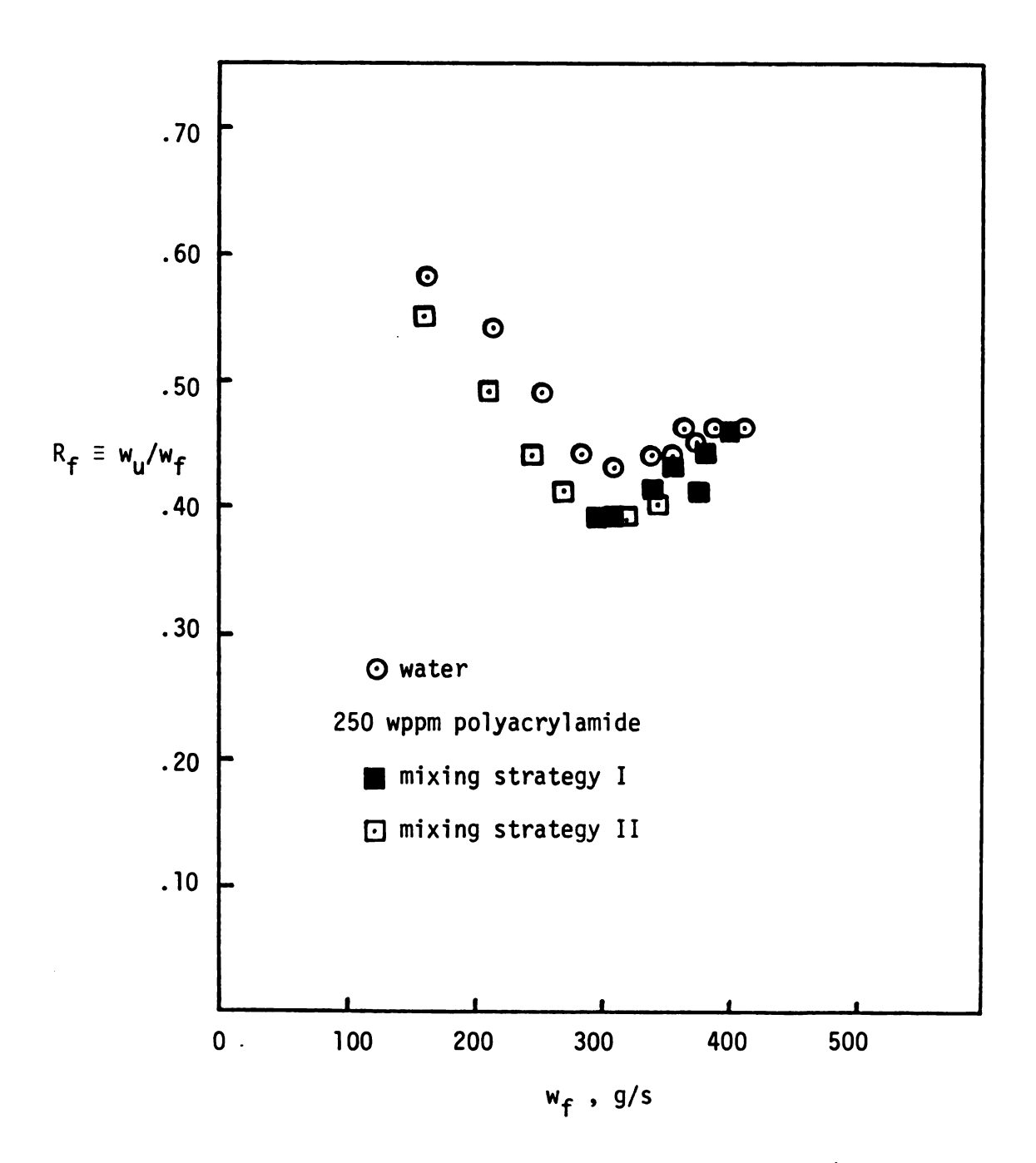


Figure 10.--The Effect of Separan AP-30 on the Flow Ratio (2 wt% clay; particle size, 0.77 microns).

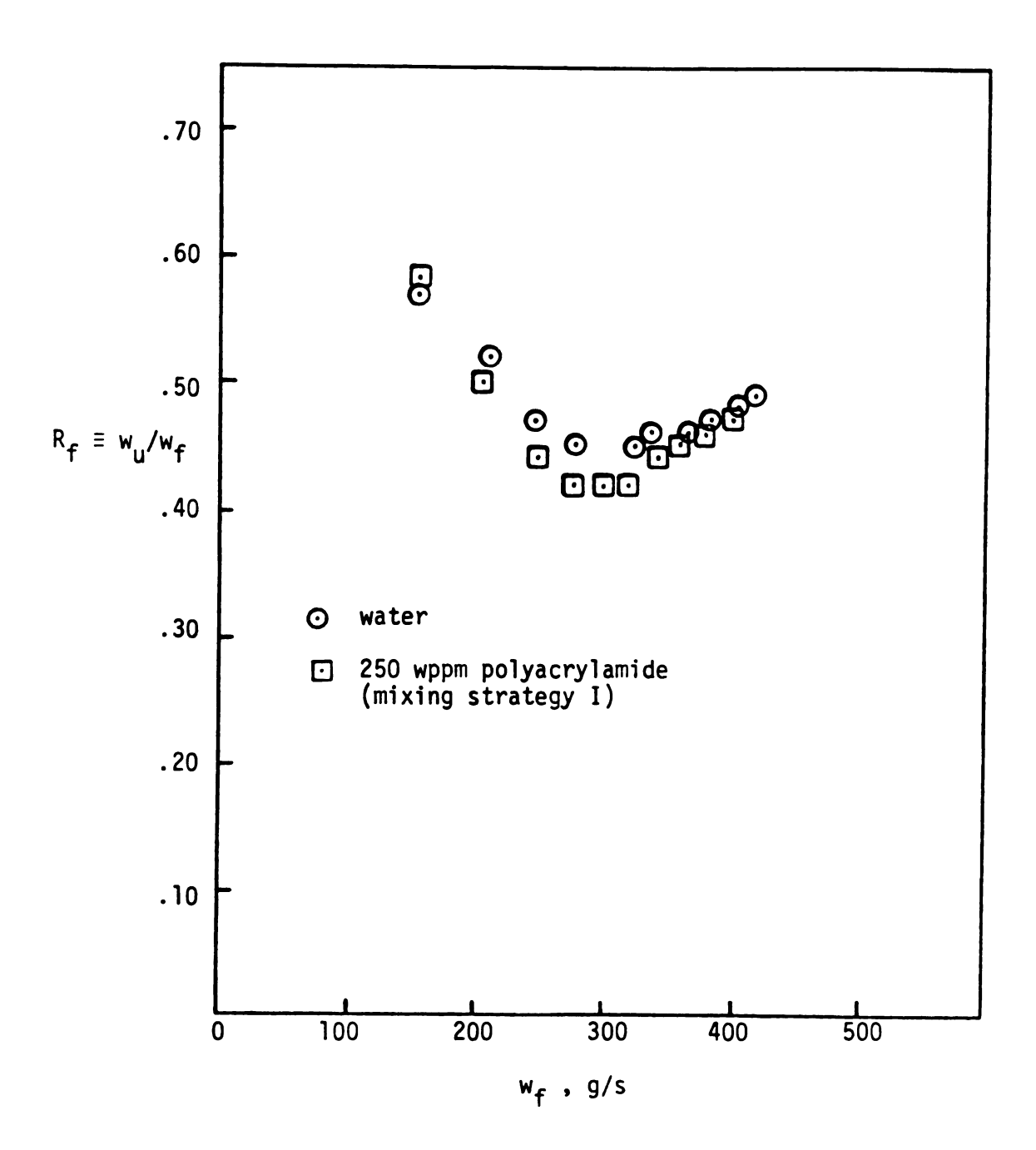


Figure 11.--The Effect of Separan AP-30 on the Flow Ratio (2 wt% clay; particle size, 10.6 microns).

with polymer addition, then an increase in R_f would occur contrary to Figure 10. Therefore, the observations regarding χ summarized by Table 1 and the tentative hypothesis that n increases, suggests that the magnitude of K is reduced by the polymer. This conjecture could be tested by measuring α experimentally.

The Effect of Polymer on the Centrifugal Efficiency of a 10mm Hydrocyclone

Figures 12, 13, and 14 illustrate the effect of the polymer on the centrifugal efficiency of the hydrocyclone. For Series I and Series III (see Appendix B), the polymer was probably mechanically degraded during the drag reduction experiments prior to being used in the hydrocyclone experiments, i.e., mixing strategy I. For these series the addition of the polymer resulted in an increase in the centrifugal efficiency of up to 27 percent. For Series II the polymer was used immediately after being dissolved (mixing strategy II). For this series the addition of the polymer resulted in a decrease in the centrifugal efficiency of up to 40 percent.

Figure 13 shows that the initial effect of doubling the polymer concentration increases the centrifugal efficiency over that of Series I and Series III. However, as indicated by Figure 13, E decreases significantly during the experiment. This may be due to polymer degradation. Surprisingly, Figure 14 shows that the addition of polymer had a negligible effect on the efficiency of the hydrocyclone separating 10 micron size clay particles.

The limited amount of data obtained in these experiments makes it difficult to postulate a mechanism through which the polymer

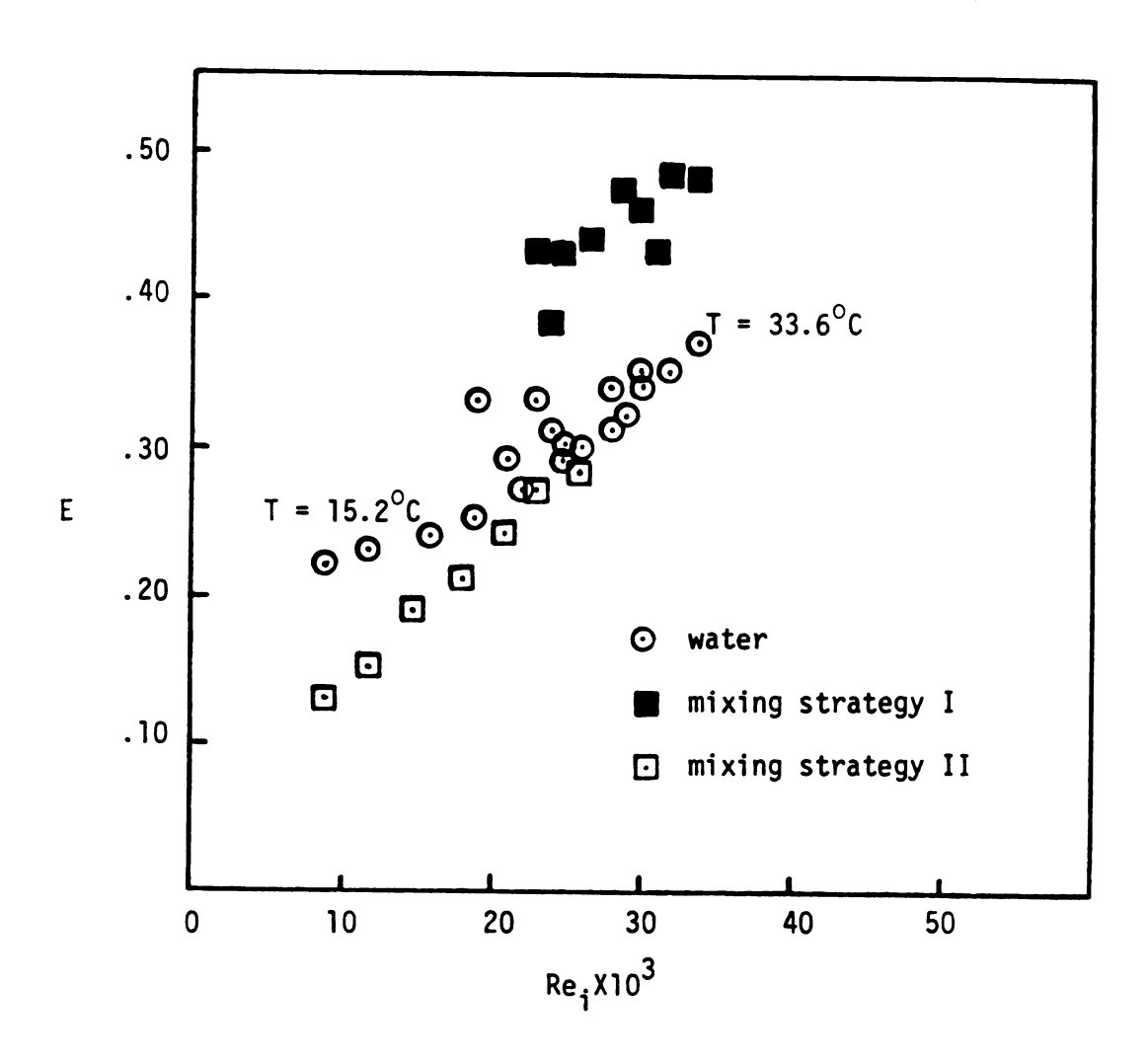


Figure 12.--The Effect of Separan AP-30 on the Centrifugal Efficiency of a 10 mm Hydrocyclone (2 wt% clay; particle size, 0.77 microns; polymer concentration, 250 wppm).

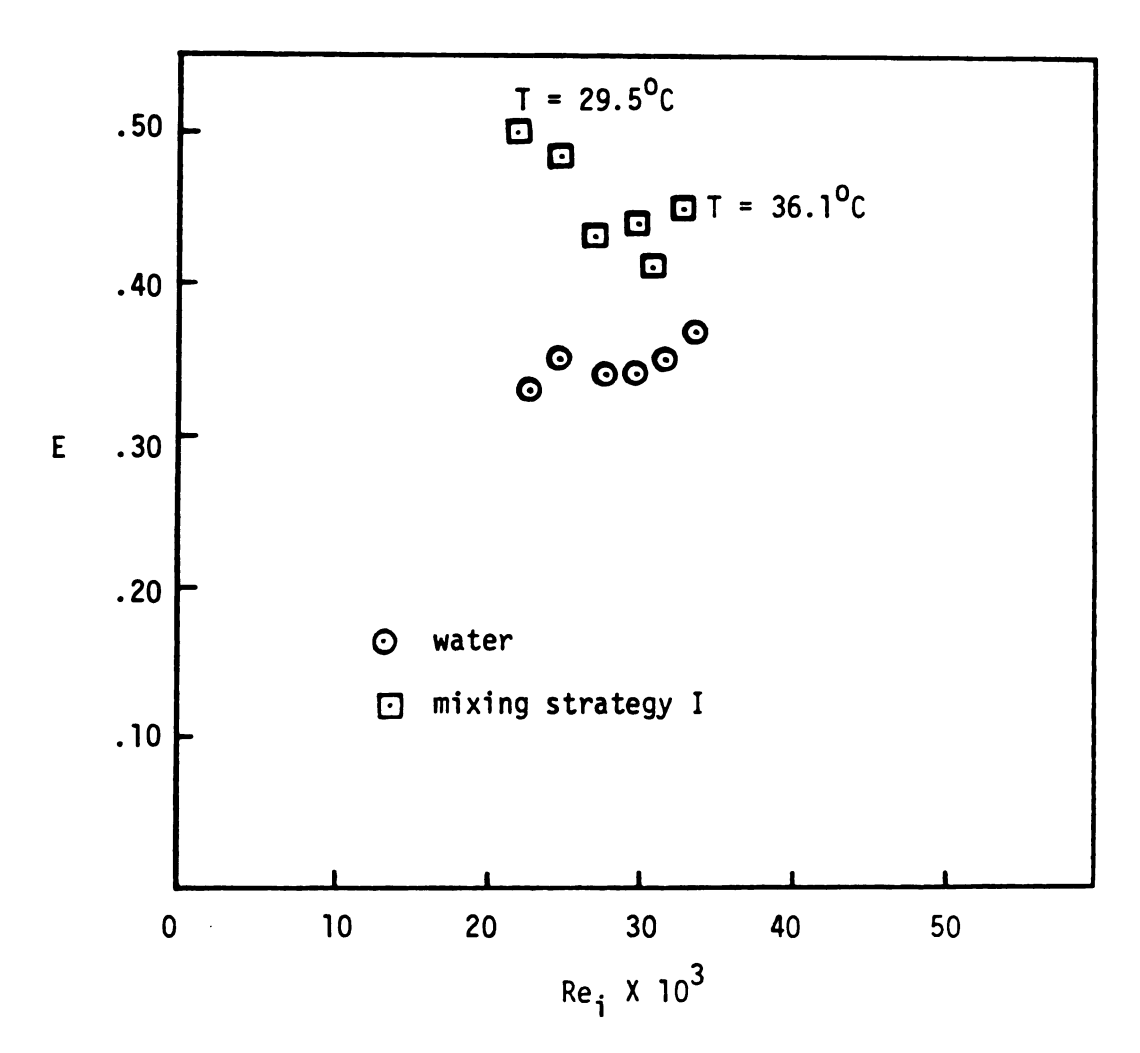


Figure 13.--The effect of Separan AP-30 on the Centrifugal Efficiency of a 10 mm Hydrocyclone (2 wt % clay; particle size, 0.77 microns; polymer concentration 500 wppm).

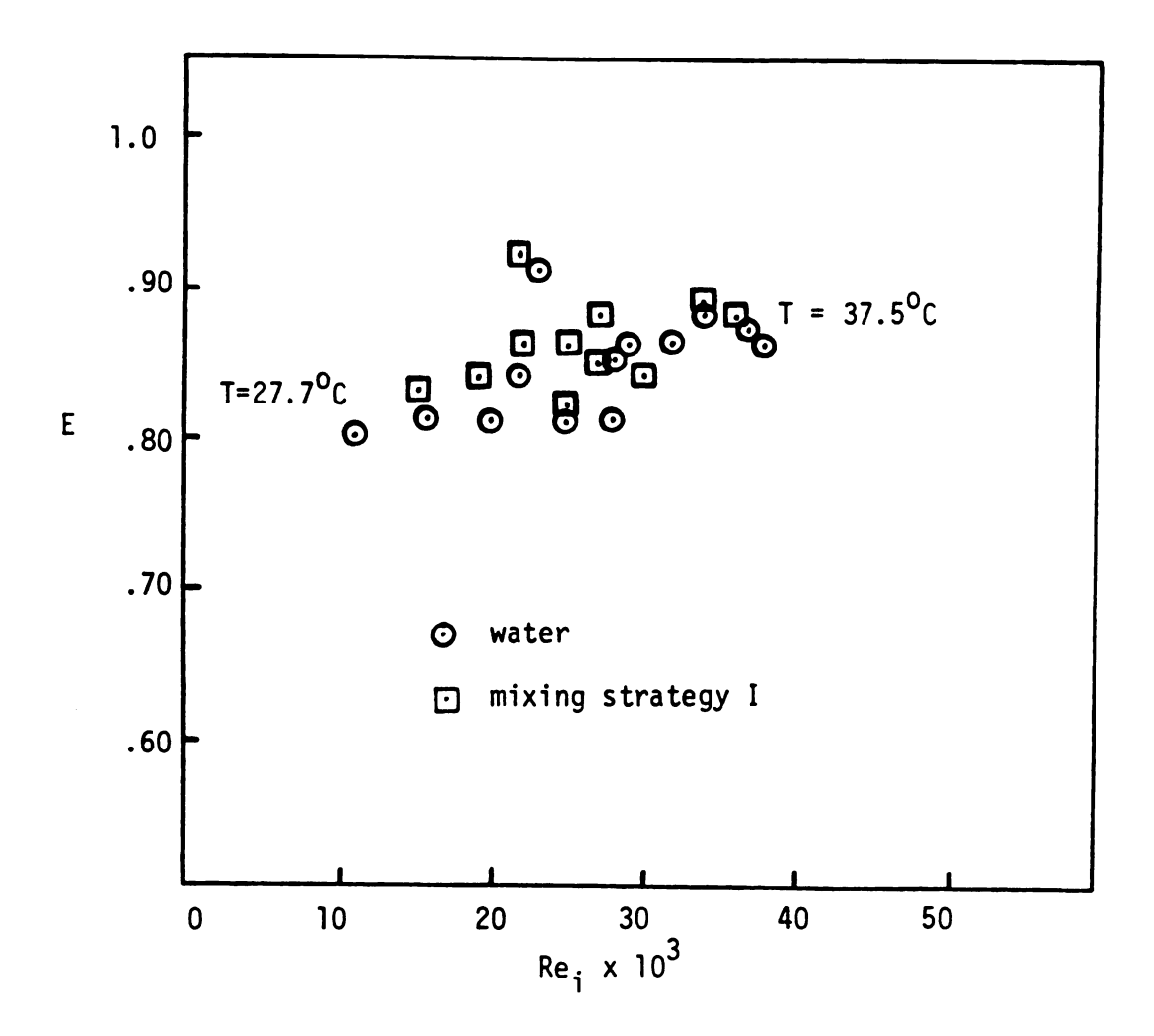


Figure 14.--The Effect of Separan AP-30 on the Centrifugal Efficiency of a 10 mm Hydrocyclone (2 wt % clay; particle size, 10.6 microns; polymer concentration 250 wppm).

affects the centrifugal efficiency. It does seem probable that the polymer somehow causes the formation of agglomerates of clay particles which are strong enough to resist the shear forces occurring in the pumps and in the hydrocyclone. Apparently, this effect is limited to the smaller particle size clay inasmuch as no effect was found for 10 micron clay particles. However, the fact that the effect depended to such a great extent on the history of the polymer solution indicates that the interaction of the polymer with the particles is much more complex than a simple agglomeration effect.

I-4. RECOMMENDATIONS FOR FURTHER RESEARCH

The apparently paradoxical results of the experiments discussed in Chapter I-3 could be better understood by carrying out experiments which include the following features:

- -Utilization of a larger transparent hydrocyclone;
- -Use of glass particles or some other appropriate substitute, instead of the Kaolinite clays used here to avoid the complications of polymer-clay interactions;
- -Measurement of the physical properties, such as apparent viscosity, of the solvent-polymer mixture so a meaningful comparison between the performance of the hydrocyclone with and without polymers can be made;
- -Determination of the significance of ionic strength, pH, etc., of the solvent on the ability of small amounts of high molecular weight polymers to alter the performance of hydrocyclones; and,
- -Study the centrifugal efficiency of the hydrocyclones for solvent-polymer mixtures which exhibit maximum drag reduction in fully developed turbulent pipe flow according to Virk's criteria (Virk, 1975).

Another useful experiment would be to measure the components of the velocity field in a hydrocyclone using laser doppler anemometry. Measurements with and without polymer additives could be made in the absence of clay or glass particles so the effect of the polymer on specific flow structures could be determined. Dye injection could also be used to identify significant qualitative differences in flow patterns caused by the polymer.

Hydrocyclones have already contributed in important ways to many industrial operations, but their full potential as inertial separators has not been reached. The problems proposed for study here should contribute to an understanding of the mechanics of separation in centrifugal fields and could lead to either new applications or improved strategies for more traditional uses.

PART II

THEORETICAL PREDICTION OF THE SEPARATIONAL EFFICIENCY OF A CYLINDRICAL HYDROCYCLONE

II-1. INTRODUCTION

Motivation

The advantages of the hydrocyclone have led to its wide-spread use as a separations device. This success has come about despite a lack of basic understanding of many aspects of the fluid mechanical processes occurring in the hydrocyclone. The motivation for development of a theoretical model of the hydrocyclone is to overcome this lack of knowledge. A natural result of a better understanding of hydrocyclone operation would be more efficient hydrocyclone utilization.

A good example of the current understanding of the physical processes occurring in the hydrocyclone can be seen in the results of Part I of this thesis. The difficulty in drawing any concrete conclusions about the effect of polymer additives on hydrocyclone operation is obvious.

Review of Theoretical Efficiency Equations in the Literature

The majority of theoretical efficiency equations are derived using one of two approaches. The approaches are similar in that both utilize the ${\rm d}_{50}$ concept and both assume that Stokes law is valid in the hydrocyclone. The differences in the two approaches arise in the assumptions made about the behavior of the solid particles in the flow field.

According to the 'equilibrium orbit' approach, particles in the hydrocyclone achieve an equilibrium orbit at a radial position where their terminal settling velocity just equals the inward liquid radial velocity. If the equilibrium orbit lies outside of the locus of zero vertical velocity, the particle is carried toward the underflow. If the equilibrium orbit lies inside the locus of zero vertical velocity, the particle leaves the hydrocyclone through the vortex finder. The particle of size \mathbf{d}_{50} achieves an equilibrium orbit coincident with the locus of zero vertical velocity.

In the "residence time" approach it is assumed that the residence time of a particle in the hydrocyclone is too short for the particle to reach its equilibrium orbit. Moreover, in order for a particle to leave the hydrocyclone through the underflow orifice, it must reach the wall of the hydrocyclone during its residence time. Thus, a particle of size ${\rm d}_{50}$ is that particle which, when entering at the center of the inlet, just succeeds in reaching the wall at the apex of the hydrocyclone.

Based on the results of dye studies, Bradley and Pulling (1959) inferred that the locus of zero vertical velocity is cylindrical in the cylindrical portion of the hydrocyclone and conical in the conical portion. Furthermore, in the cylindrical portion there is no inward radial velocity so that stratification of the particles takes place only in the conical section. Using this physical evidence, Bradley developed an equilibrium orbit approach

for estimating ${\rm d}_{50}$ by equating the terminal settling velocity of the ${\rm d}_{50}$ size particle to the average radial velocity across the locus of zero vertical velocity (see page 84 in Bradley, 1965). Using the residence time approach, Rietema (1961) developed a different expression for ${\rm d}_{50}$. Although these empirical expressions for ${\rm d}_{50}$ are useful for correlating data, they give little insight into the physical processes occurring in the hydrocyclone.

An alternate theoretical approach was taken by Bloor and Ingham (1973) which can best be described by referring to Figure 15. Figure 15 shows the trajectory of a particle of size 'a' which reaches its equilibrium line at point P. Point P is the intersection of the locus of zero vertical velocity and the equilibrium line of the particle. The equilibrium line is the locus of positions where the centrifugal and drag forces acting on the particle of size 'a' balance. Bloor assumed that particles of size 'a' between A and B will reach their equilibrium line before crossing the locus of zero vertical velocity and, thereby will exit through the under-Similarly, particles of size 'a' between A and the air core will reach their equilibrium line after crossing the locus of zero vertical velocity and thus, will leave through the vortex finder. Bloor further assumed that the suspension is completely homogeneous at the level of the vortex finder so that the efficiency of the hydrocyclone for a particle of size 'a' would simply be the fraction of the total flux of fluid passing through the annular region between A and B.

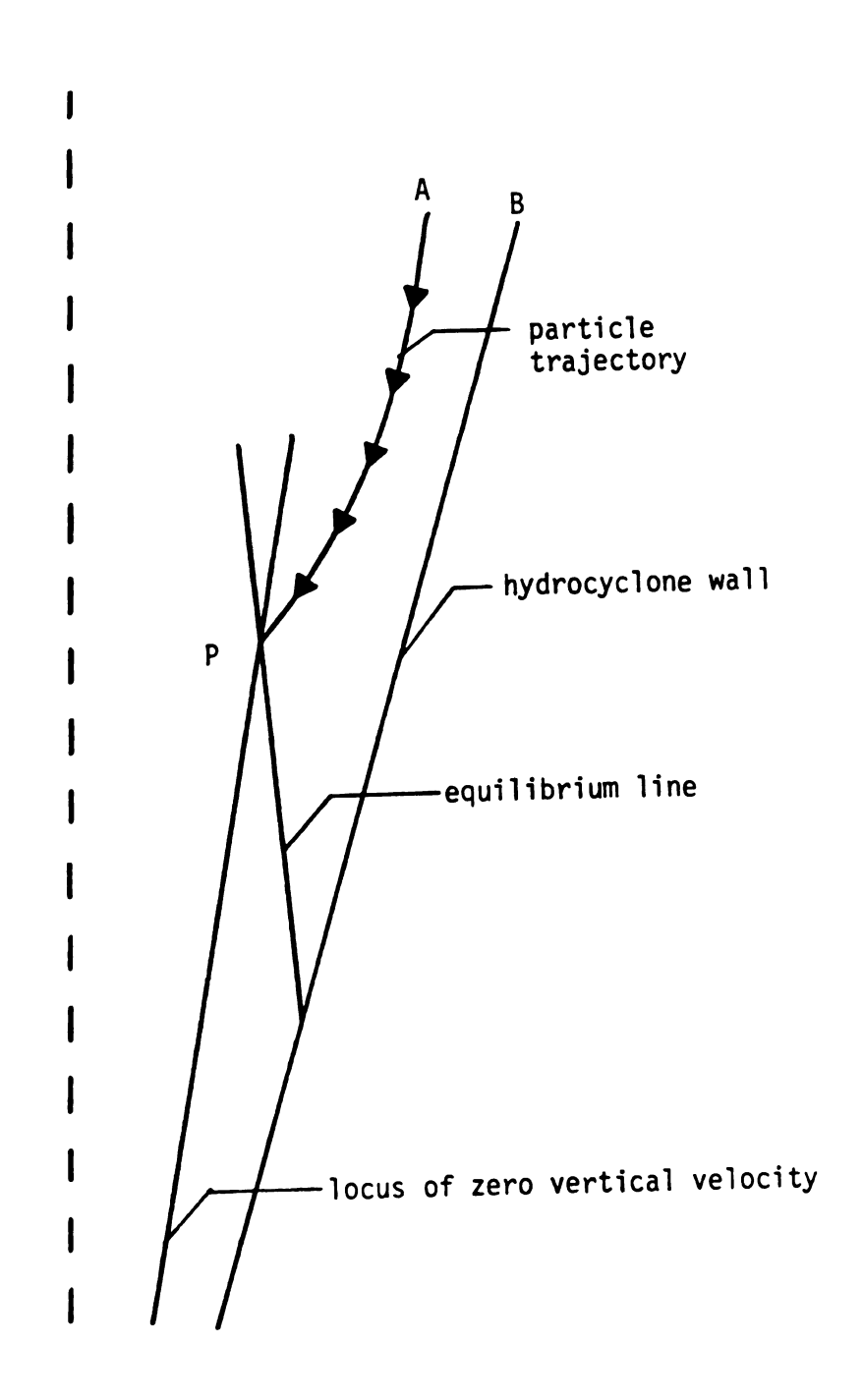


Figure 15.--Path of a Particle of Size 'a' in a Conical Hydrocyclone.

Bloor developed approximate expressions for the velocity by using an inviscid model. He also derived a differential equation for the trajectory of a particle of size 'a' which could be numerically integrated to obtain the coordinates of point A. Although Bloor's work contains more fluid mechanics than either Bradley's or Rietema's, he justifies his approximate solution for the velocity components by comparing his theoretical results with the data of Kelsall, which are limited in scope and which have been recently criticized by Knowles, et al. (1973).

<u>Objectives</u>

The purpose of Part II of this thesis is to develop a mathematical model to obtain insight into the physical processes occurring in a cylindrical hydrocyclone. Although the geometry of a cylindrical hydrocyclone differs from the normal conical one, the flow structures and mode of operation are similar for both. For instance, separation of solid particles occurs as a result of a centrifugal force field and the reversal of the vertical velocity results in the formation of an inner and outer spiral as well as a locus of zero vertical velocity in both cases.

A model will be developed using an approach similar to that of Bloor. However, an exact solution of the equation of motion will be used. While some of the more complicated aspects of the flow profile will be ignored in the development of the model, the model will, nevertheless, provide a basic framework which will be able to account for the effects of the important flow structures on the efficiency of hydrocyclones.

II-2. FORMULATION OF THE MODEL

Fluid Mechanics in a Cylindrical Hydrocyclone

The velocity components of an ideal fluid (ρ = a constant, μ = 0) in cylindrical coordinates (r, θ , z) will be determined in this section and will also be used to determine the path of a solid particle in a cylindrical hydrocyclone. The geometry of the problem is illustrated in Figure 16. All the fluid which enters the hydrocyclone exits through the vortex finder. A simplifing assumption is made that there is no short circuit flow in the upper regions of the hydrocyclone and there is no air core.

The flow in the hydrocyclone is assumed to be at steady state and to be irrotational. That is, the vorticity,

$$\mathbf{w} \equiv \nabla \mathbf{u} \tag{2-1}$$

is zero. The physical significance of this can best be understood by considering an infinitesimal packet of fluid as it moves through the hydrocyclone. In irrotational flow, the packet of fluid does not rotate around its own axis as it moves through the hydrocyclone. Obviously, this assumption cannot hold near the axis of the hydrocyclone or in the viscous boundary layer.

For steady state, the equation of motion for an ideal fluid is (see p. 80 in Bird, et al., 1960)

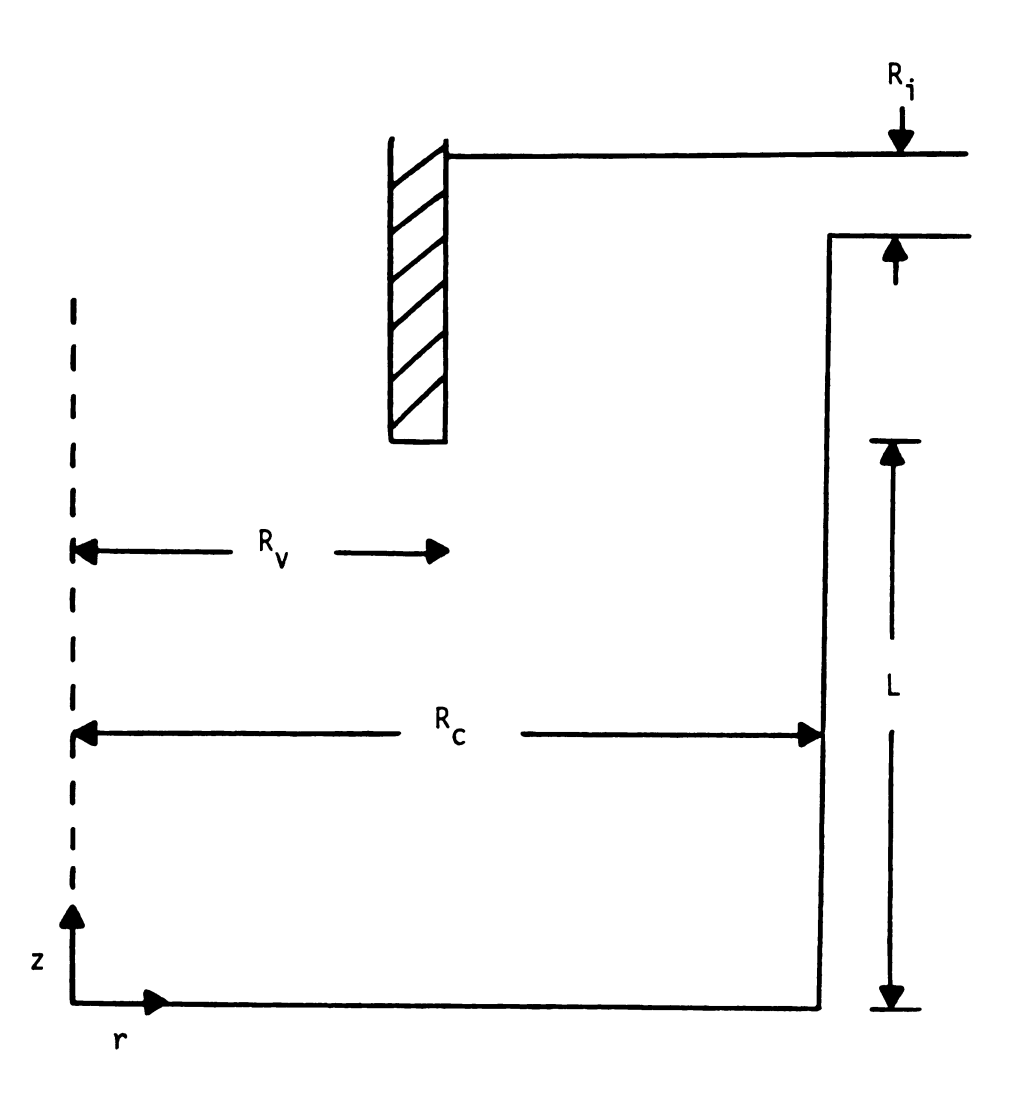


Figure 16.--Parameters Used to Describe the Performance of a Cylindrical Hydrocyclone.

$$\rho \mathbf{u} \cdot \nabla \mathbf{u} = -\nabla P . \tag{2-2}$$

For axisymetric flow, ρ and \underline{u} are independent of θ . Therefore, u_{θ} satisfies

$$u_{r} \frac{\partial u_{\theta}}{\partial r} + \frac{u_{r}u_{\theta}}{r} + u_{z} \frac{\partial u_{\theta}}{\partial z} = 0.$$
 (2-3)

An exact solution to equation (2-3) is

$$r u_{\theta} (r) = constant \equiv A.$$
 (2-4)

This is the tangential velocity for a free vortex and does not hold throughout the spatial domain of a hydrocyclone. As discussed in Part I of this thesis, numerous workers with both gas cyclones and hydrocyclones have determined that

$$u_{\theta} = \frac{A}{r^{n}} \tag{2-5}$$

where n normally has values between 0.5 and 1 (Bradley, 1965). Both equation (2-4) and equation (2-5) hold only in those regions away from the axis of the hydrocyclone. Near the axis the flow is approximately solid body rotation, which implies that $\mathbf{u}_{\theta} \propto \mathbf{r}$.

The constant in equation (2-4) can be determined by considering \boldsymbol{u}_{θ} at the feed inlet. Here

$$u_{\theta} (R_{c}) = \frac{Q}{A_{i}} = u_{i}$$
 (2-6)

where Q is the volumetric feed flow rate and $A_{\dot{1}}$ is the cross sectional area of the inlet. Therefore,

$$A = u_i R_C . (2-7)$$

The equation of continuity in cylindrical coordinates for an incompressible fluid is

$$\frac{1}{r}\frac{\partial}{\partial r}(r u_r) + \frac{\partial u_z}{\partial z} = 0.$$
 (2-8)

Equation (2-8) can be satisfied exactly by introducing a stream function ψ (r, z) related to u_r and u_z as follows (see page 131 in Bird, et al., 1960):

$$u_n = -1/r \partial \psi/\partial z \tag{2-9}$$

$$u_{7} = 1/r \partial \psi / \partial r . \qquad (2-10)$$

The components of the vorticity, defined by equation (2-1), are

$$w_{\theta} = \frac{\partial u_{\mathbf{r}}}{\partial z} - \frac{\partial u_{\mathbf{z}}}{\partial r}$$
 (2-11)

$$w_{r} = \frac{1}{r} \frac{\partial u_{z}}{\partial \theta} - \frac{\partial u_{\theta}}{\partial z}$$
 (2-12)

$$w_z = \frac{1}{r} \frac{\partial}{\partial r} (r u_\theta) - \frac{1}{r} \frac{\partial u_r}{\partial \theta}$$
 (2-13)

For axisymetric flow and u_{θ} defined by equation (2-4), w_{r} and w_{z} are zero. Since $\underline{w}=\underline{0}$ by assumption, w_{θ} must also equal zero. Thus,

$$\frac{\partial u_{\mathbf{r}}}{\partial z} - \frac{\partial u_{\mathbf{z}}}{\partial r} = 0. \tag{2-14}$$

Inserting equations (2-9) and (2-10) into equation (2-14) gives

$$\frac{\partial^2 \psi}{\partial x^2} + r \frac{\partial}{\partial r} \frac{1}{r} \frac{\partial \psi}{\partial r} = 0.$$
 (2-15)

The flux of material through the walls of the hydrocyclone must be zero, so

$$u_r(R_c, z) = 0$$
 (2-16)

and

$$u_{z}(r, 0) = 0.$$
 (2-17)

According to equations (2-9) and (2-10) these boundary conditions are satisfied for

$$\frac{\partial \psi}{\partial z} (R_C, z) = 0 \qquad (2-18)$$

and

$$\frac{\partial \psi}{\partial r} (r, 0) = 0. \qquad (2-19)$$

Equations (2-18) and (2-19) indicate that the value of ψ at the boundaries is an arbitrary constant, which can be conveniently set to zero. Note that for this model the velocity at the wall has a non trivial tangential component, which can be interpreted as the velocity just outside the viscous boundary layer.

Because all of the fluid entering the hydrocyclone must flow through the region between the outer wall of the vortex finder and the wall of the hydrocyclone,

$$Q = -2\pi \int_{R_{V}}^{R} u_{z}(r, L) r dr.$$
 (2-20)

Substituting equation (2-10) into equation (2-20) and integrating gives

$$-2\pi \left[\psi(R_{c}, L) - \psi(R_{v}, L)\right] = Q.$$
 (2-21)

As discussed earlier, $\psi(\mbox{\bf R}_{_{\mbox{\bf C}}}$, L) is zero so equation (2-21) reduces to

$$\psi(R_{V}, L) = \frac{Q_{F}}{2\pi}$$
 (2-22)

 $\psi(r, z)$ satisfies the following boundary value problem:

$$\frac{\partial^2 \psi}{\partial z^2} + r \frac{\partial}{\partial r} \frac{1}{r} \frac{\partial \psi}{\partial r} = 0 \qquad (2-23)$$

with boundary conditions

$$\psi = 0$$
, at $r = R_c$ (2-24a)

$$\psi = 0$$
, at $z = 0$ (2-24b)

$$\psi = Q/2\pi$$
, at $r = R_v$, $z = L$. (2-24c)

The solution can be constructed by separation of variables and is given by

$$\psi (r, z) = \frac{Q}{2\pi} \frac{r J_1 (\lambda r) \sinh (\lambda z)}{R_V J_1 (\lambda R_V) \sinh (\lambda L)}$$
 (2-25)

where λ is a constant. From boundary condition (2-24a), it follows that λR_c is a zero of J_1 (λR_c).

Substituting equation (2-25) into equation (2-9) gives,

$$u_{r} = -\frac{Q}{2\pi} \frac{\lambda J_{1}(\lambda r) \cosh(\lambda z)}{R_{v} J_{1}(\lambda R_{v}) \sinh(\lambda L)}.$$
 (2-26)

Note that at $r=R_C$ and r=0, $u_r=0$. Because the fluid enters the hydrocyclone at R_C and leaves through the vortex finder, the radial velocity is negative throughout the hydrocyclone. In practice, regions of positive radial velocities have been found in the upper regions of hydrocyclones (Bradley, 1965). This corresponds to the formation of recirculating eddies as discussed in Part I of this thesis. For the purposes of this model, however, it will be assumed that there is no secondary flow features so the radial velocity is negative everywhere. This implies that λR_C is the first zero of J_1 (λR_C). Thus

$$\lambda \equiv \frac{\beta_1}{R_C} \tag{2-27}$$

where β_1 is the first zero of J_1 (λR_c).

Inserting equation (2-25) into equation (2-10) gives,

$$u_{z} = \frac{Q}{2\pi} \frac{\lambda J_{o} (\lambda r) \sinh (\lambda z)}{R_{v} J_{1} (\lambda R_{v}) \sinh (\lambda L)}$$
 (2-28)

Note that at $r = R_c$, u_z is nonzero for 0 < z < L, and at z = 0, $u_z = 0$ for $0 < r < R_c$. The locus of zero vertical velocity is a cylinder of radius R_o , coaxial with the hydrocyclone. R_o can be calculated from

$$J_{O}(\lambda R_{O}) = 0. \qquad (2-29)$$

With

$$\beta_{0} \equiv \lambda R_{0} = \beta_{1} \frac{R_{0}}{R_{c}} , \qquad (2-30)$$

the ratio of R_0 to R_c is determined by the first zeroes of J_0 (*) and J_1 (*), viz.,

$$\frac{R_0}{R_c} = \frac{\beta_0}{\beta_1} \simeq \cdot 63 \tag{2-31}$$

This a priori prediction compares favorably with the dye studies of Bradley (1959) which imply that $R_{\rm O} \simeq .43~R_{\rm C}$.

Particulate Mechanics

The horizontal movement of solid particles as they pass through a hydrocyclone is governed by the relative magnitude of two opposing forces acting on the particle. The centrifugal force arising from the motion of the fluid tends to propel the particle toward the wall of the hydrocyclone, while the drag force on the particle tends to resist any movement of the particle relative to the fluid. One of the key assumptions in trajectory calculations

is that these forces are balanced throughout the hydrocyclone (see Bloor and Ingham, 1973). Thus with the centrifugal force on a particle of radius 'a' and of density ρ_S given by

$$F_c = \frac{4}{3} \pi a^3 (\rho_s - \rho) (u_\theta^2)/r$$
 (2-32)

and the drag force given by Stokes law

$$F_d = 6\pi \mu a(u_{pr} - u_r)$$
 (2-33)

then $F_d = F_c$ implies that

$$(\rho_s - \rho) 4/3 \pi a^3 (u_\theta^2)/r = 6\pi \mu a (u_{pr} - u_r)$$
. (2-34)

Thus, the horizontal velocity of the particle, u_{pr} , is

$$u_{pr} = u_r + \frac{(\rho_s - \rho) 4/3 \pi a^3 u_\theta^2}{6\pi \mu a r}$$
 (2-35)

This result, employed by Bradley and others, is not strictly applicable to all situations; however, it is of considerable value in predicting the behavior of solid particles in hydrocyclones. For a detailed discussion of the underlying physical assumptions implied in equation (2-35) see Bradley (1965).

The tangential and vertical velocities of the particle and the fluid are assumed to be equal. Because u_{pr} and u_{pz} do not depend on time explicitly, the particle position r_p can be written in terms of the radial and axial components of the particle velocity as follows:

$$\frac{dr_p}{dt} = \frac{dr_p}{dz_p} \frac{dz_p}{dt}$$
 (2-36)

or

$$\frac{dr_p}{dz_p} = \frac{u_{pr}}{u_{pz}} \qquad . \tag{2-37}$$

Equation (2-37) can be used to determine the trajectory of a particle as it approaches its equilibrium line. Combining equations (2-4), (2-5), (2-26), and (2-35) yields

$$u_{pr} = \frac{(\rho_s - \rho)(4/3)\pi a^3 u_i^2}{6\pi \mu a R_c} (\frac{R_c}{r})^3$$

$$-\frac{Q}{2\pi}\frac{\lambda}{R_{v}}\frac{J_{1}(\lambda r_{p})\cosh(\lambda z_{p})}{J_{1}(\lambda R_{v})\sinh(\lambda L)}.$$
 (2-38)

Equation (2-28) gives u_z as an explicit function of r and z. Therefore with $u_{pz} = u_z$,

$$u_{pz} = \frac{Q}{2\pi} \frac{\lambda J_0 (\lambda r_p) \sinh (\lambda z_p)}{R_v J_1 (\lambda R_v) \sinh (\lambda L)} . \qquad (2-39)$$

Efficiency Calculations

A strategy for calculating the efficiency of a cylindrical hydrocyclone for particles of any given size can be developed based on the foregoing results. The first step is to find the point of intersection of the particle equilibrium line with the locus of zero vertical velocity (point $(z_e/L, R_o/R_c)$ in Figure 17). The trajectory of the particle can then be determined by integrating back

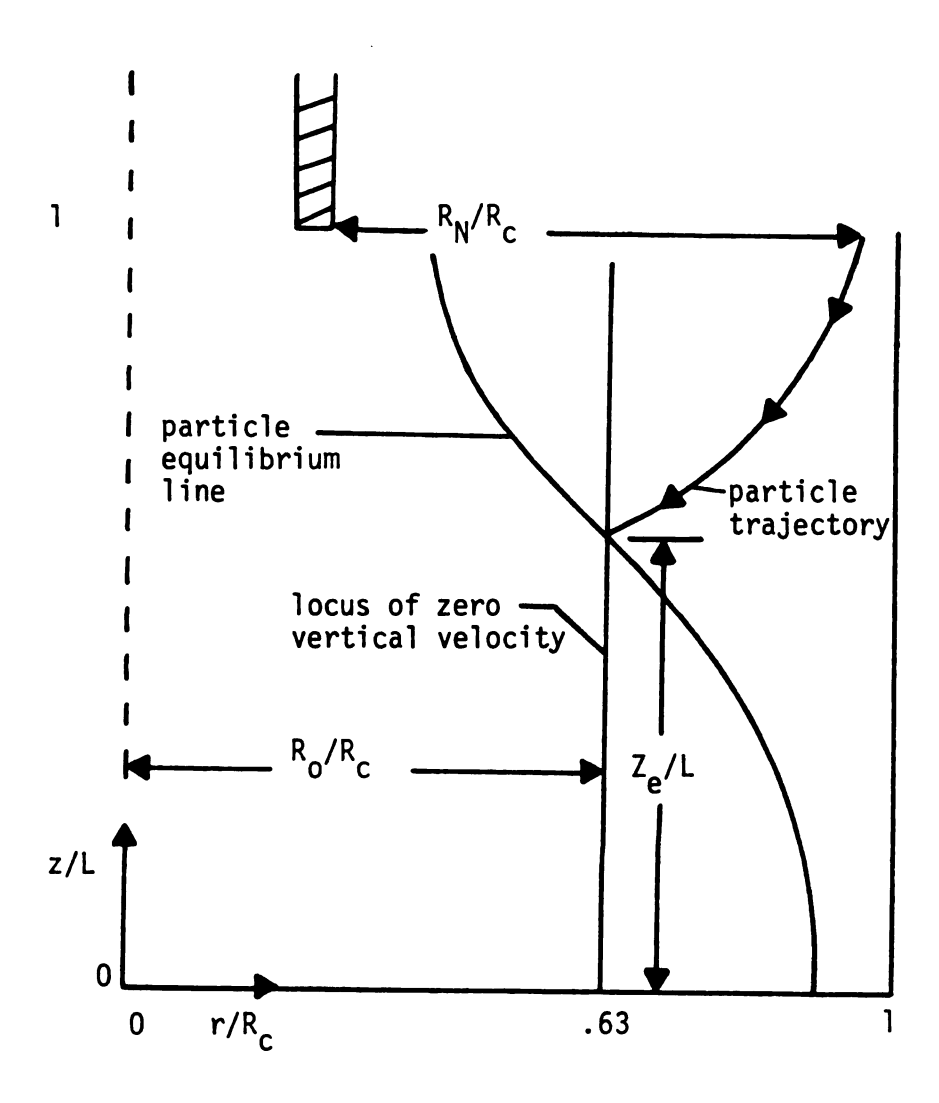


Figure 17.--Coordinate System and Path of a Particle of Size 'a' in a Cylindrical Hydrocyclone.

along its path from the point of intersection to the level of the vortex finder (z/L = 1 in Figure 17). This critical trajectory separates the particle paths into two sets: those which cross their equilibrium line before the zero vertical velocity lines; and, those which cross the zero vertical velocity line first. At z = L, the distribution of the particles is assumed to be homogeneous. This is a reasonable assumption because experimental evidence has shown that a region of severe turbulence exists above this level (Rietema, 1961). The radial position of the critical particle path at z/L = 1 is denoted by R_N/R_C in Figure 17.

All particles of the given size with radial positions at z/L=1 greater than R_N/R_C will reach their equilibrium line outside of the locus of zero vertical velocity. These particles will then be entrained in the downward moving fluid and will eventually reach the walls of the hydrocyclone where they are removed from the system. All particles with radial positions at z/L=1 less than R_N/R_C will reach their equilibrium lines inside of the locus of zero vertical velocity. These particles will be entrained in the upward moving fluid and thus are not separated by the hydrocyclone. Therefore, because the distribution of particles at z/L=1 is homogeneous, the efficiency of the hydrocyclone for particles of a given size is that fraction of the total flux of the suspension which passes through the annular region between R_N/R_C and $r/R_C=1$.

The equilibrium line of the particle can be found by setting $u_{\tt pr}$ equal to zero in equation (2-38). The locus of zero

vertical velocity is given by equation (2-31). The coordinates of the intersection of the two lines must satisfy

$$\frac{\left(\rho_{s}-\rho\right)(4/3)\pi a^{3} u_{i}^{2}}{6\pi \mu a R_{c}} \left(\frac{R_{c}}{R_{o}}\right)^{3}$$

$$= \frac{Q \lambda}{2\pi R_{v}} \frac{J_{1}(\lambda R_{o}) \cosh(\lambda z_{e})}{J_{1}(\lambda R_{v}) \sinh(\lambda L)} . \qquad (2-40)$$

It is convenient to rewrite equation (2-40) in dimensionless form. This can be accomplished by using equation (2-27) and equation (2-30) together with the dimensionless variables

$$\xi \equiv z/L$$
 (2-41a)

$$\eta \equiv r/R_{c} \tag{2-41b}$$

$$N = \frac{A_c}{A_i} \frac{2}{\beta_i} \left(\frac{R_c}{R_0}\right)^3 \frac{(\rho_s - \rho)(4/3)\pi a^3 (u_i^2/R_c)}{6\pi \mu a u_i}$$
 (2-41c)

N measures the relative importance of centrifugal and viscous forces within the hydrocyclone. For industrial applications N ranges from 4×10^{-5} to 40. Equation (2-40) can now be written as

$$N = \frac{J_1 (\beta_0) \cosh (\beta_1 \xi_e G)}{J_1 (\beta_1 \eta_v) \sinh (\beta_1 G)} \frac{1}{\eta_v}$$
 (2-42)

where G is L/R_c . Solving equation (2-42) for ξ_e gives

$$\xi_{e} = \frac{\cosh^{-1}\left[\frac{\eta_{v}^{N} J_{1} (\beta_{1} \eta_{v}) \sinh (\beta_{1} G)}{J_{1} (\beta_{0})}\right]}{G\beta_{1}}. (2-43)$$

Inserting equation (2-38) and equation (2-39) into equation (2-37) and using equation (2-42) gives

$$\frac{d\eta_{p}}{d\xi_{p}} = \left(\frac{\eta_{p}}{\eta_{p}}\right)^{3} \frac{J_{1}(\beta_{1}\eta_{o}) \cosh (\beta_{1}\xi_{e} G) - J_{1} (\beta_{1}\eta_{p}) \cosh (\beta_{1}\xi_{p})}{J_{o} (\beta_{1}\eta_{p}) \sinh (\beta_{1}\xi_{p} G)}. (2-44)$$

The value of η_N (i.e., $r_P = R_N$ at z = L) can be determined by numerically integrating equation (2-44) from ξ_e to $\xi = 1$. However, at the intersection point (η_0, ξ_e) both the numerator and denominator of equation (2-44) are zero. By expanding equation (2-44) about the point (η_0, ξ_e) it can be shown that the initial slope of the trajectory is

$$\frac{d\eta_{P}}{d\xi_{P}}\Big|_{\eta = \eta_{O}} = 1 + \frac{2}{\beta_{O} \tanh (\beta_{1} \xi_{e} G)}$$

$$\xi = \xi_{e}$$
(2-45)

An expression for the centrifugal efficiency can now be written as

$$E = \frac{\int_{\eta_{N}}^{1} u_{z} \eta d\eta}{\int_{\eta_{V}}^{1} u_{z} \eta d\eta}$$
 (2-46)

Inserting equation (2-10) into (2-46) and integrating yields

$$E = \frac{\psi(\eta_{N}, 1)}{\psi(\eta_{V}, 1)}$$
 (2-47)

which, according to equation (2-25) can be rewritten as

$$E = \frac{\eta_{N}}{\eta_{V}} = \frac{J_{1} (\beta_{1} \eta_{N})}{J_{1} (\beta_{1} \eta_{V})} . \qquad (2-48)$$

Although equation (2-48) is rigorous within the context of the model, it does not account for some important flow phenomena intrinsic in hydrocyclone operations. Specifically, the effects of an air core and secondary flows in the upper regions of the hydrocyclone are ignored. Coupling this model with a boundary layer analysis could provide additional insight into factors influencing the efficiency of hydrocyclones.

II-3. DISCUSSION OF RESULTS AND CONCLUSIONS

Computer Program

The computer program described in this section was used to determine the behavior of the mathematical model developed in Chapter II-2. The program calculates the centrifugal efficiency of a cylindrical hydrocyclone in terms of specific geometrical and operating variables. The range over which these variables were studied included values representative of the experiments described in Part I as well as those estimated in industrial scale applications.

A block diagram of the computer program is shown in Figure 18. After $n_{\rm V}$, G, and N are set, $\xi_{\rm e}$ is calculated using equation (2-43). The program calculates the initial slope of equation (2-44) using equation (2-45). $n_{\rm N}$ is calculated by integrating equation (2-44) using a second order Runga-Kutta method from $\xi = \xi_{\rm e}$ to $\xi = 1$. Once the value of $n_{\rm N}$ is calculated, the efficiency is determined by equation (2-48).

The program output can be conveniently divided into three cases defined by Table 2. Table 2 shows the range of parameters studied.

Table 2.--Parameters Specified for Model Studies.

Geometric	Parameters Characteristic of Experiments in Part I Parameter $A_c/A_i = 13.09$									
Physical parameters										
Solids de	ensity		2.58 g/ml							
Particle	size		.77 microns	- 10.6 microns						
Viscosity	′		1.1 cp6	88 cp						
Operating	g variable	u _i = 152 - 417 g/sec								
	Values	of Dimension in Model S	nless Groups U Studies	Ised						
Group	Case Study I	Case Study II	Case Study III	Nominal Range for 10 mm Hydrocyclone						
N	0 - 1.5	.82	. 82	9 x 10 ⁻⁴ 7						
G	2	2	.4 - 2	14.8						
$\eta_{oldsymbol{V}}$.63	163	.63	.25						

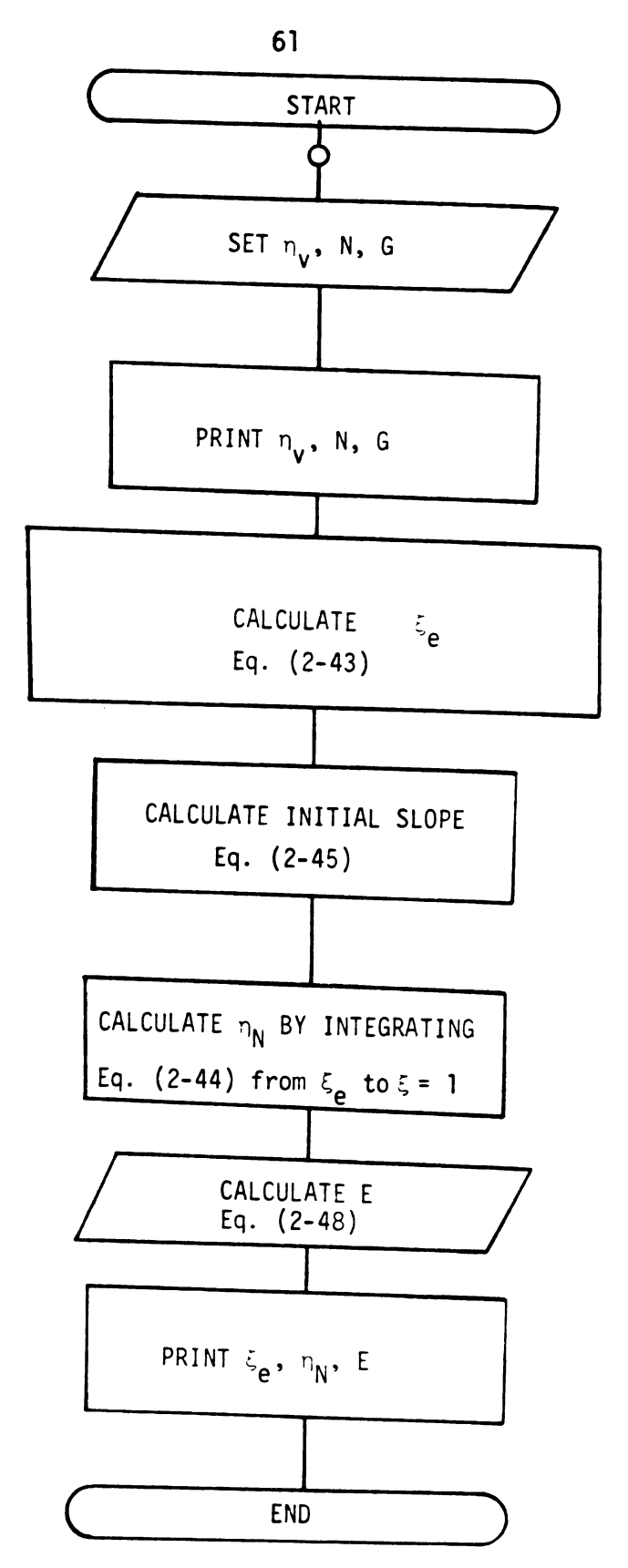


Figure 18.--Block Diagram of Computer Program.

Case Study I: The Effect of N on the Centrifugal Efficiency of a Cylindrical Hydrocyclone

Figure 19 shows that increasing the value of N results in an increase in the centrifugal efficiency of a cylindrical hydrocyclone. The mechanism through which the model reflects the increase in efficiency with increasing N originates in equation (2-43). Equation (2-43) reveals that an increase in N results in an increase in ξ_e . The increase in ξ_e results in a decrease in η_N as can be seen by inspecting Figure 17. The decrease in η_N in turn results in an increase in E as indicated by equation (2-48).

The definition of N (equation (2-41c)) reveals that N can be increased by increasing a, u_i , or the density difference (ρ_s - ρ). It has been found that the efficiency of hydrocyclones used in industrial applications is also increased when these parameters are increased (see Chapter 8 in Bradley, 1965). N can also be increased by increasing the value of (A_c/A_i). The effect of increasing efficiency with decreasing inlet diameter has been demonstrated experimentally by Kelsall (1953). Bradley (1965) gives an optimum value of the inlet diameter based on considerations of the velocity reduction factor α . In the model equations, α is ignored so that the efficiency continues to increase as the inlet diameter is decreased.

The results of the experiments in Part I of this thesis also show an increase in centrifugal efficiency with an increase in N. For the experiments using the smaller particle size clay, N

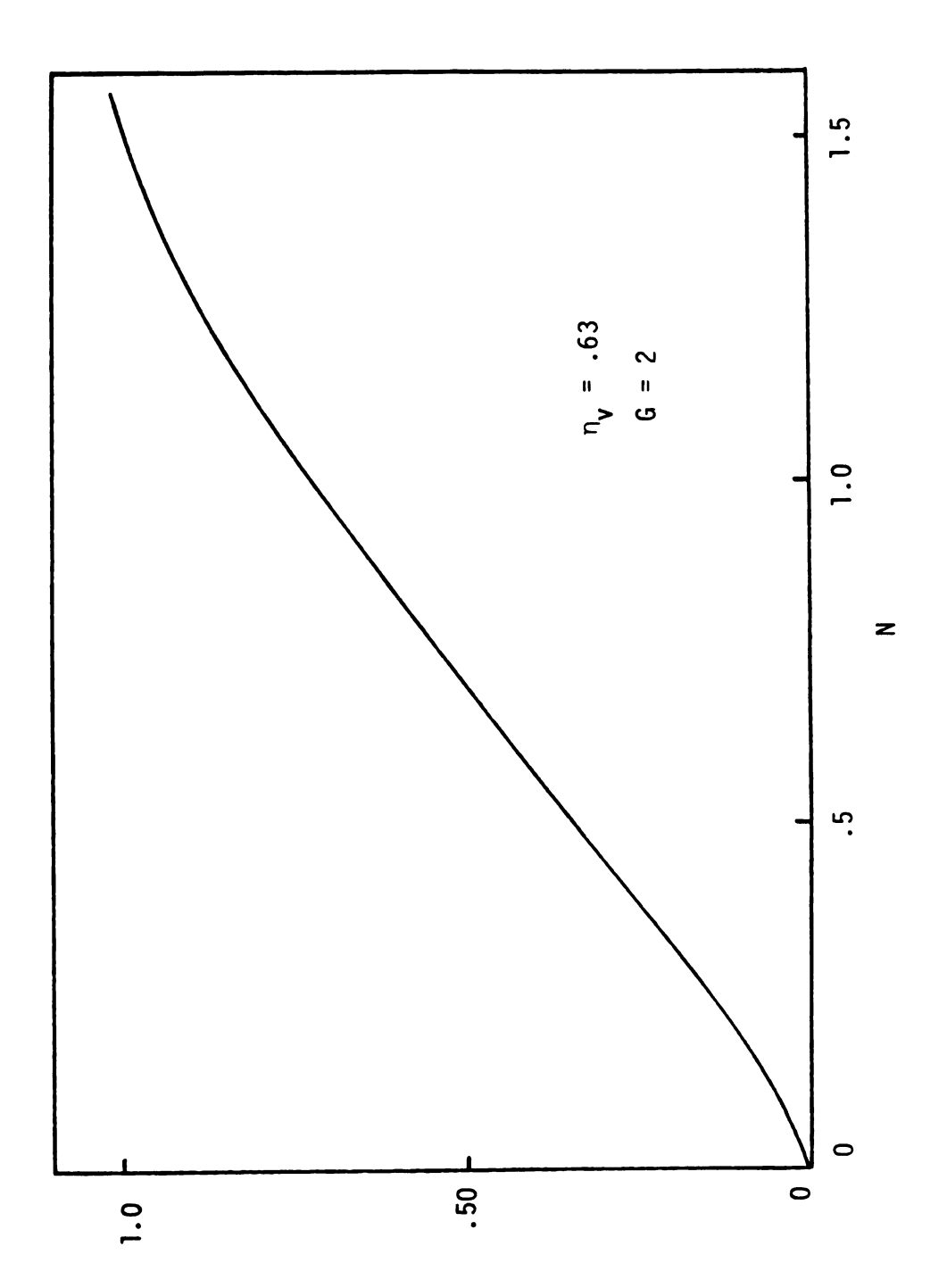


Figure 19.--The Effect of Increasing N on the Centrifugal Efficiency of a Cylindrical Hydrocyclone.

ranges from 8.9 to 10^{-4} to 3.1×10^{-3} with an increase in the efficiency from .22 to .37. For the experiments using the larger particle size clay, N ranges from .2 to .7 with an increase in E from .80 to .86.

Case Study II: The Effect of n_v on the Centrifugal Efficiency of a Cylindrical Hydrocyclone

Figure 20 shows that the efficiency of a cylindrical hydrocyclone increases as the diameter of the vortex finder is increased up to a value of .63 $R_{\rm C}$. Beyond this value the efficiency decreases, although this is not indicated on Figure 20.

Figure 20 can be understood by examining the effect of $\eta_{_{\boldsymbol{V}}}$ on the velocity components. The radial and vertical velocities are decreased as the value of $R_{_{\boldsymbol{V}}}$ is increased because of the presence of the function $R_{_{\boldsymbol{V}}}$ J_{1} $(\lambda R_{_{\boldsymbol{V}}})$ in the denominator of the right hand side of equation (2-26) and equation (2-28). The function has a maximum value at $R_{_{\boldsymbol{V}}}=(\beta_1/\beta_0)$ $R_{_{\boldsymbol{C}}}$, or $R_{_{\boldsymbol{V}}}=.63$ $R_{_{\boldsymbol{C}}}$ (see Figure 21). Thus, if $R_{_{\boldsymbol{V}}}$ exceeds this value, the magnitude of $u_{_{\boldsymbol{V}}}$ and $u_{_{\boldsymbol{Z}}}$ increase again. Now, as the radial velocity decreases, the drag force on a particle in its equilibrium orbit decreases. Since $u_{_{\boldsymbol{\theta}}}$ does not depend on the location of the vortex finder, the centrifugal force field is independent of $\eta_{_{\boldsymbol{V}}}$. Therefore, if $F_{_{\boldsymbol{d}}}$ decreases because $\eta_{_{\boldsymbol{V}}}$ increases then the equilibrium orbit (defined by $F_{_{\boldsymbol{d}}}=F_{_{\boldsymbol{C}}}$) must shift toward the outer wall of the hydrocyclone. Inspection of Figure 17 will reveal that the result of the shift in the equilibrium locus

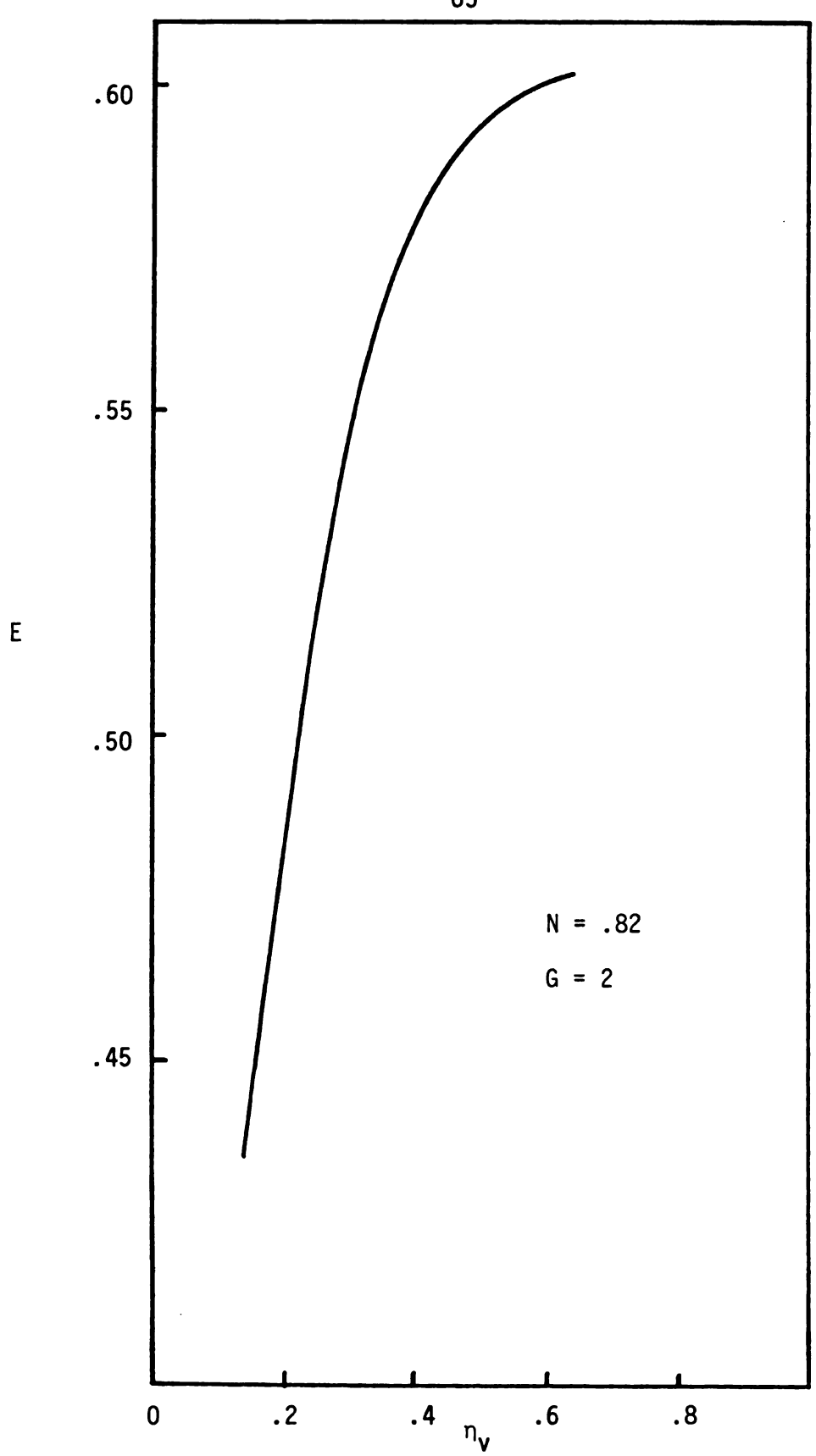


Figure 20.--The Effect of Increasing η_V on the Centrifugal Efficiency of a Cylindrical Hydrocyclone.

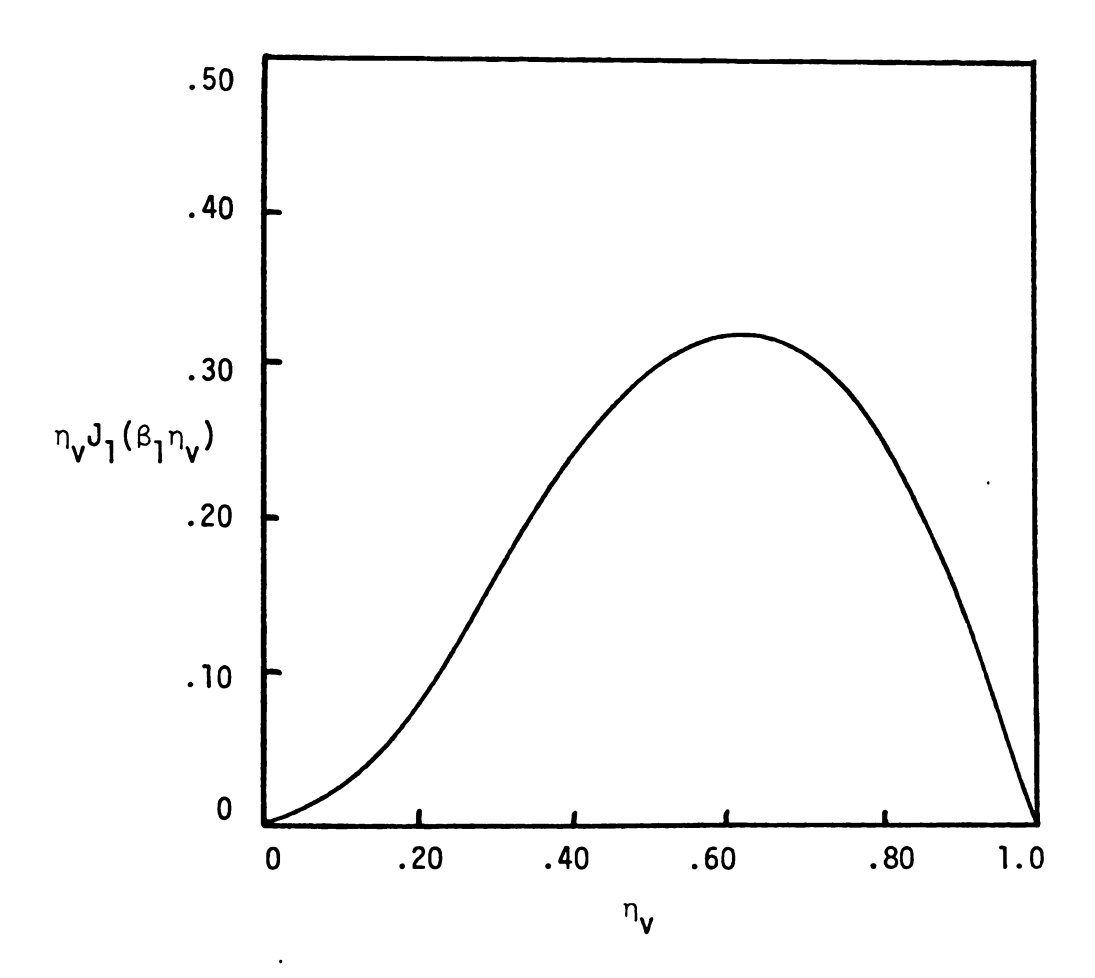


Figure 21.--The Effect of η_{v} on η_{v} J_{1} $(\beta_{1}\eta_{v})$ for β_{1} = 3.83.

will be to move the intersection of the equilibrium line and the locus of zero vertical velocity toward the top of the hydrocyclone.

Equation (2-38) indicates that, as $R_{_{\mbox{$V$}}}$ is increased the magnitude of $u_{_{\mbox{$T$}}}$ is also increased. Because the magnitude of $u_{_{\mbox{$Z$}}}$ is decreased as $R_{_{\mbox{$V$}}}$ is increased, the trajectory of the particle becomes more horizontal. This has the effect of increasing $\eta_{_{\mbox{$N$}}}$. However, the computer program indicates for the values of $\eta_{_{\mbox{$N$}}}$ studied that the effect of increasing $\xi_{_{\mbox{$E$}}}$ has a greater effect on $\eta_{_{\mbox{$N$}}}$ than the effect of the particle trajectory so that the value of $\eta_{_{\mbox{$N$}}}$ decreases as the value of $\eta_{_{\mbox{$V$}}}$ is increased. The decrease in $\eta_{_{\mbox{$N$}}}$ leads to an increase in E as discussed in Case Study I. The general conclusion is that the efficiency increases as the diameter of the vortex finder increases up to the diameter of the locus of zero vertical velocity.

Using dye studies, Bradley (1959) also found that increasing the vortex finder diameter beyond the locus of zero vertical velocity causes an increase of the inward radial flow of the fluid and a concomitant decrease in efficiency. The effect of changing the vortex finder diameter of hydrocyclones used for industrial applications has a significant effect on the short circuit flow which carries particles directly from the inlet to the vortex finder. To balance the adverse effects of the inward radial velocity and the short circuit flow, Bradley (1965) recommends that $n_{\rm v}$ should be .13 to .43.

Case Study III: The Effect of G on the Centrifugal Efficiency of a Cylindrical Hydrocyclone

The effect of increasing the length is to increase the efficiency of a cylindrical hydrocyclone. This effect is most pronounced for values of G less than 1.00 and becomes less apparent as the value of G is increased above 2.0. The output of the computer program which illustrates these points is presented in Figure 22.

Equation (2-43) reveals that the effect of increasing G is to increase ξ_e . Furthermore, this effect becomes less significant as G becomes greater than 2.0. The result of increasing ξ_e is an increase in E as discussed earlier.

Although the length is one of the least well defined aspects of the design of hydrocyclones, an increase in efficiency with increasing length has been demonstrated by several workers (Bradley, 1965). Dahlstrom (1949) also demonstrated that this effect diminishes as the length is increased excessively.

Conclusions and Recommendations for Further Research

The results of the computer study illustrate that the simplified model developed here can make a priori predictions of the performance of a hydrocyclone in terms of important design and operating variables. A close connection with actual performance data cannot be expected until the influences of the air core, the short circuit flow, and the viscous boundary layers are incorporated.

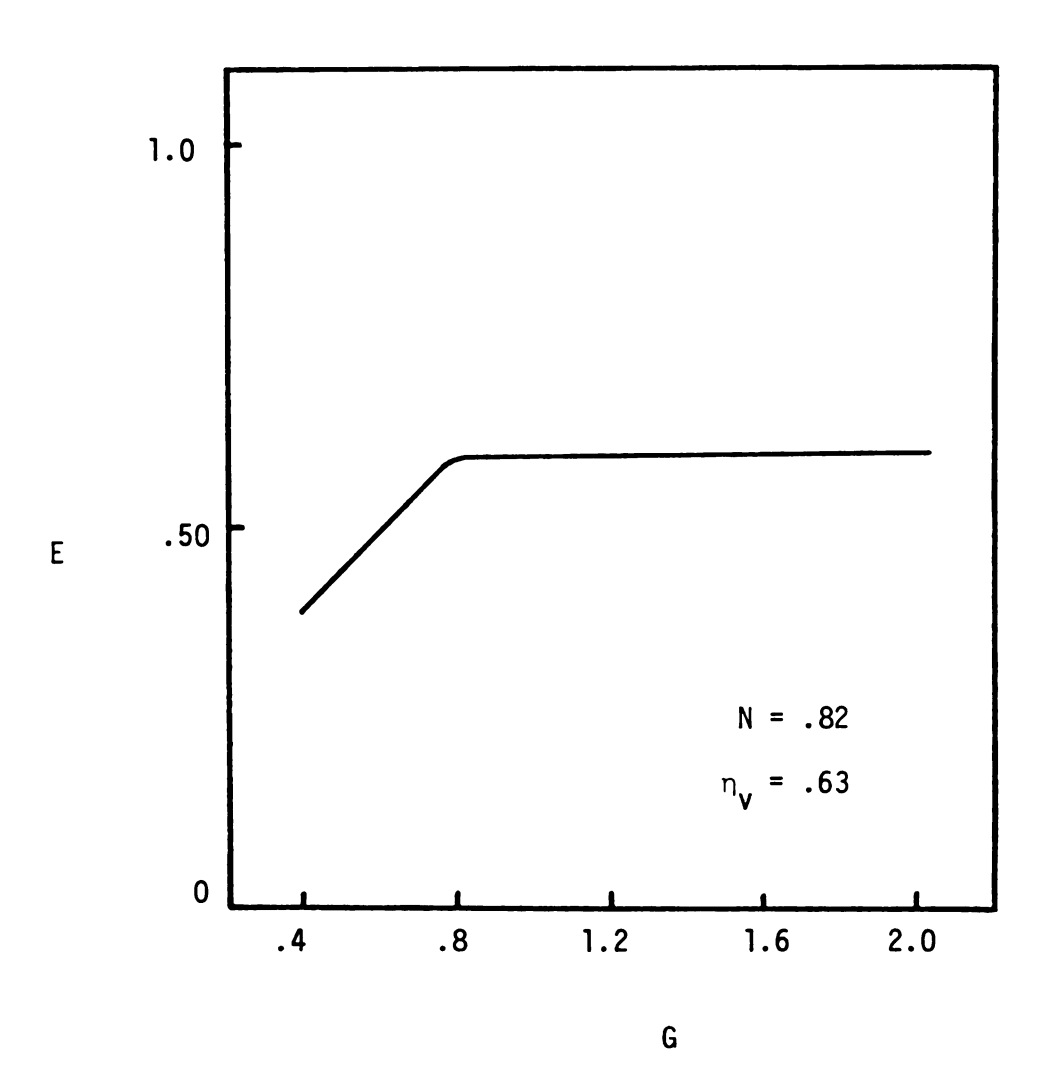


Figure 22.--The Effect of Increasing G on the Centrifugal Efficiency of a Cylindrical Hydrocyclone.

Thus, what has been provided is a prototype for further development.

In order for the model developed here to provide significant insight into the observed behavior of hydrocyclones the equations should be developed for a conical hydrocyclone. The data obtained from the experiments proposed in Chapter I-4 of Part I could be combined with the model equations to gain an understanding of how the various flow structures in the hydrocyclone affect the centrifugal efficiency. In particular, the structures and influences of the viscous boundary layer, the short circuit flow, and the air core could be understood by carrying out an approximate integral-type analysis (see,e.g., Bloor and Ingham, 1976). The results of the proposed experiments involving polymer additives could also be used in conjunction with the model equations to provide a basic understanding of the mechanism through which the polymer affects the flow structure and centrifugal efficiency of the hydrocyclone.

APPENDIX A EXPERIMENTAL DATA ON DRAG REDUCTION IN PIPE FLOW

Table A-1.--Experimental Data for Fully Developed Flow of a Newtonian Fluid in a Circular Tube. (D=3/16 in.; L=5 ft.; ρ = 62.4 lb. $_{\rm m}$ /ft³)

(o _C)	ΔP (PSI)	w (lb _m /sec)	μ (cp)	Re	f						
Series I											
16.3 18.2 20.4 22.5 24.4 26.5	3.7 .105 8.1 .145 12.4 .180 16.8 .212 21.1 .239 25.4 .263		1.102 1.050 .995 .947 .906	11500 16700 21900 27100 32000 36900	.0056 .0064 .0064 .0062 .0061						
		Seri	es II								
15.2 17.4 19.3 21.0 22.9 24.9	3.7 8.3 12.5 16.8 21.1 25.4	8.3 .149 12.5 .180 16.8 .212 21.1 .240		11200 16900 21400 26200 31000 35900	.0056 .0062 .0064 .0062 .0061						
		Serie	es III								
15.8 17.4 19.0 20.5 22.7 24.6	3.9 8.3 12.5 16.8 21.2 25.5	.103 .147 .178 .207 .236 .264	1.117 1.072 1.030 .993 .942 .902	11100 16600 21000 25300 30300 35400	.0061 .0064 .0066 .0065 .0063						

Table A-2.--Experimental Data for Fully Developed Flow of a 252 ppm Polyacrylamide Solution in a Circular Tube. (D=3/16 in.; L = 5 ft.; ρ = 62.4 lb_m/ft³)

(o _C)	ΔP (PSI)			Re	f
		Seri	es I		
16.0 18.2 20.0 22.4 24.4 26.6	3.9 8.2 12.6 17.0 21.4 25.7	3.2 .170 3.6 .214 3.0 .244 3.4 .275		13600 19600 25900 31200 36700 43000	.0042 .0047 .0046 .0047 .0047
		Seri	es II		
17.3 19.1 21.4 23.5 25.5 27.3	3.9 8.3 12.6 17.0 21.4 25.7	.128 .178 .219 .248 .279 .304	1.075 1.027 .972 .925 .883 .849	14400 21000 27300 32500 38200 43400	.0040 .0043 .0044 .0046 .0046
		Serie	es III		
15.4 17.1 18.9 21.0 22.8 24.4	3.9 8.3 12.6 17.0 21.3 25.7	.130 .175 .208 .238 .270	1.128 1.080 1.032 .981 .940	14000 19600 24400 29400 34800 39800	.0038 .0045 .0049 .0050 .0049

Table A-3.--Experimental Data for Fully Developed Flow of a 500 ppm Polyacrylamide Solution in a Circular Tube. (D=3/16 in.; L = 5 ft.; ρ = 62.4 lb_m/ft³)

(o _C)	ΔP (PSI)	w (lb _m /sec)	μ (cp)	Re	f
18.7	4.0	.151	1.037	17600	.0029
20.5	8.5	.208	. 993	25400	.0033
22.5	12.9	.251	. 947	32100	.0034
24.2	17.3	.293	.910	39100	.0033
25.5	21.7	.322	.883	44200	.0035
27.2	26.1	. 351	.851	50000	.0035

APPENDIX B

EXPERIMENTAL DATA ON SOLID-LIQUID SEPARATIONS IN A 10MM HYDROCYCLONE

Table B-1.--Performance Data of 10mm Hydrocyclone. (2 wt. % clay in water, mean particle size = .7 microns. D_i = .106 in.)

	Underflow Overflow			Fe	ed				
ΔP (PSI)	(o _C)	(1b _{m/} sec)	conc. (wt%)	(1b _m /sec)	conc. (wt%)	w (1b _m / sec)	conc. (wt%)	Rei	Ε
				Ser	ies I				
50 60 70 80 90	16.6 19.5 22.5 24.6 26.6 28.0	.339 .349 .366 .381 .406	2.492 2.461 2.505 2.508 2.543 2.534	. 384 . 401 . 434 . 459 . 483 . 483	1.233 1.281 1.291 1.275 1.261 1.209	.723 .750 .800 .840 .889	1.825 1.846 1.839 1.845 1.848 1.815	19000 21000 24000 26000 29000 30000	.33 .29 .31 .30 .32
				Ser	ies II				
10 20 30 40 50 60 70	15.2 17.3 20.1 22.8 25.6 28.1 30.0	.209 .256 .271 .277 .302 .324 .348	2.324 2.394 2.490 2.619 2.669 2.711 2.750	.150 .216 .284 .351 .385 .417 .439	1.655 1.590 1.571 1.501 1.464 1.416 1.375	. 358 . 472 . 555 . 628 . 687 . 741 . 787	2.014 2.007 1.994 1.996 1.988 1.984 1.986	9000 12000 16000 19000 22000 25000 28000	.22 .23 .24 .25 .27 .29
				Seri	es III				
50 60 70 80 90 100	27.5 28.8 30.5 31.6 33.5 33.6	.296 .322 .343 .367 .392 .418	2.764 2.855 2.823 2.805 2.834 2.829	. 385 . 413 . 436 . 453 . 467 . 484	1.332 1.323 1.328 1.311 1.328 1.291	.681 .735 .779 .820 .859	1.949 1.972 1.981 1.975 2.009 1.981	23000 25000 28000 30000 32000 34000	.33 .35 .34 .34 .35

Table B-2.--Performance Data of 10mm Hydrocyclone. (2 wt.% clay in 252 ppm Polyacrylamide solution, mean particle size = .7 microns. D_i = .106 in.)

4.0		Under			flow	_	ed	Rei	E
ΔP (PSI)	(° _C)	(1b _m / sec)	conc. (wt%)	(1b _m /sec)	conc. (wt%)	(1b _m /sec)	conc. (wt%)	1	_
				Ser	ies I				
70 80 90 100	26.5 29.1 29.9 31.2	.302 .335 .369 .385	2.818 2.835 2.785 2.699	.450 .454 .469 .476	.909 .997	.752 .789 .838 .861	1.807 1.785 1.754 1.772	24000 27000 29000 31000	.38 .44 .47 .43
				Ser	ies II				
10 20 30 40 50 60 70	14.8 17.8 20.5 22.8 25.3 27.5 29.0	.193 .226 .236 .245 .256 .275 .303	2.122 2.241 2.422 2.522 2.600 2.693 2.691	.158 .233 .300 .354 .397 .428 .454	1.768 1.652 1.575 1.538 1.485 1.435 1.378	.351 .459 .536 .599 .653 .703	1.925 1.953 1.949 1.941 1.911 1.909	9000 12000 15000 18000 21000 23000 26000	.13 .15 .19 .21 .24 .27
				Seri	es III				
50 60 70 80 90	29.8 31.5 32.5 34.0 34.6 35.3	.252 .272 .303 .335 .336 .394	3.267 3.189 3.148 3.060 2.979 2.905	. 394 . 422 . 439 . 448 . 460 . 471	1.131 1.121 1.095 1.067 1.011	.646 .694 .742 .783 .826 .865	1.958 1.924 1.925 1.904 1.868 1.855	23000 25000 27000 30000 32000 34000	.43 .43 .44 .46 .48

Table B-3.--Performance Data of 10mm Hydrocyclone. (2 wt.% clay in 500 ppm Polyacrylamide Solution, mean particle size = .7 microns. D_i = .106 in.)

=======	A-1-2 - 1-2-	Underflow		0ver	Overflow		Feed		
ΔP (PSI)	(° _C)	w (1b _m / sec)	conc. (wt%)	W (1b _m / sec)	conc. (wt%)	w (1b _m / sec)	conc. (wt%)	Rei	E
50	29.5	.252	3.413	.387	.987	.639	1.946	22000	.50
60	31.5	.267	3.321	.423	1.072	.690	1.927	25000	.46
7 0	33.3	.280	3.251	.434	1.112	.714	1.958	27000	.43
80	34.5	.311	3.170	.457	1.102	.768	1.934	30000	.44
90	35.5	. 337	3.084	.464	1.108	.801	1.980	31000	.41
100	36.1	.363	3.042	.473	1.092	.836	1.933	33000	.45

Table B-4.--Performance Data of 10mm Hydrocyclone. (2 wt.% clay in water, mean particle size = 10.6 microns. D_i = .106 in.)

△P (PSI)	⊤ (° _C)	Under W (1b _m / sec)	conc. (wt%)	Over W (1b _m / sec)	flow conc. (wt%)	Fe w (1b _m / sec)	ed conc. (wt%)	Re _i	E
10	27.7	. 194	3.119	.145	.463	.339	1.957	11000	.80
20	29.5	.240	3.407	.223	. 385	.463	1.950	16000	.81
30	31.4	.257	3.779	.287	.338	.544	1.993	20000	.81
40	33.2	.277	4.012	.334	.282	.611	1.912	23000	.91
50	34.8	.319	4.032	.395	.311	.714	1.964	28000	. 85
60	35.2	.338	3.937	.398	.302	.736	1.960	29000	.86
70	36.5	.370	3.957	.436	.300	.806	1.971	32000	.86
80	36.9	. 393	3.903	.450	.282	.843	1.948	34000	.88
90	37.5	.427	3.839	.468	.279	.895	1.968	37000	.87
100	37.5	.446	3.691	.473	.272	.919	1.934	38000	.86
50	24.2	.346	3.677	.355	.391	.701	1.976	22000	.84
60	26.3	.365	3.706	.399	.369	.764	1.971	25000	.81
70	28.5	.383	3.728	.429	.339	.812	1.974	28000	.80

Table B-5.--Performance Data of 10mm Hydrocyclone. (2 wt.% clay in 252 ppm Polyacrylamide Solution, mean particle size = 10.6 microns. D_i = .106 in.)

		Under	flow	0ver	flow	Fe	ed		
ΔP (PSI)	(° _C)	(1b _w / sec)	conc. (wt%)	W (1b _W / sec)	conc. (wt%)	(1b _W /sec)	conc. (wt%)	Re i	E
10	27.2	.193	3.064	.142	. 459	.335	1.936	11000	.80
20	28.9	.223	3.532	.223	.378	.446	1.929	15000	.83
30	30.7	.237	4.007	.305	.360	.542	1.925	19000	.84
40	32.0	.253	4.270	.355	.334	.608	1.942	22000	. 86
50	33.5	.274	4.157	.381	.315	.655	1.940	25000	.82
60	34.9	.297	4.185	.408	.296	.705	1.936	27000	.85
70	35.6	.328	4.095	.425	.294	.753	1.958	30000	.84
80	36.5	.355	3.986	.440	.263	.795		32000	
90	37.2	. 389	3.902	.448	.253	.837	1.925	34000	.89
100	37.3	.411	3.833	.468	.238	.879	1.919	36000	.88
50	25.5	.323	3.828	.35 8	.335	.681	1.896	22000	. 92
60	27.5	. 335	3.853	.409	.329	.744	1.882	25000	.86
7 0	29.5	. 365	3.807	.423	.290	.7 88	1.886	27000	.88

APPENDIX C

COMPUTER PROGRAM

```
PROGRAMIRAJECT (INPUT, OUTPUT)
C
           FROGRAM FOR CASE STUDY III
             PFAL WMMSJD MMRSJ1
SINH(X)=(EYP(F)=EYP(-X))/2
COSH(X)=(EXF(X)+FXP(-X))/2
TAMH(Y)=SINH(X)/COSH(X)
F3(7)=G+(1,+2,/(Z)+TAMH(71+G+Z)))
F1(F,Z)=G+((70/(Z1+R))+3)+COSH(71+G+ZE)+RJ1-COSH(Z1+G+Z)+FJ2)
F2(Z)=SINH(Z1+G+Z)/FZ(Z)
F3(F,Z)=F1(P,Z)/FZ(Z)
           INFUT OF OPFRATIONAL AND GEOMETRIC VARIABLES, 71=86TA1,7(=8FTA TYRSJI(.) AND PMESJA(.) ARE SUBROUTINES THAT CALCULATE J1(.) AND J3(.). AN=N, W= FTA V , 6=6.
             71=7.83171

27=2.40482

PC=70/21

V=7'/21

SJ3=PMRSJ1(21*V,IFR)

RJ1=PMRSJ1(77,IER)

AH= P2

PRINT1U,V,AY

PRINT2

DC6r=1,5

G=.4+K
             CALCULATE 25 FROM N, ETA V AND G USING ES (2-43)
             P=V+AN+SI*H(Z*+F)+PJR/PJ1
IF(B.LE.1.)GOTO5
ZE=ALOG(R+SGRT((P++Z)-1))/(G+Z1)
             INTEGRATE FROM Z=ZE TO Z=1 USING SECOND CADER RUNGA-KUTTA METHOD AND EQ(2-45) TO CBTAIN THE INITIAL SLIPE
             N=(1.-7F)/25.
P1=P'+H+F')(7E)/2.
Z=7E+H/2.
RJO=MMBSJ')(Z1+R1,IFR)
RJ2=MMBSJ')(Z1+R1,IFR)
RJC=MH+F'(P1,Z)
D01I=1,49
RJC=MMSJC(Z1+R,IFR)
RJC=MMSJC(Z1+R,IFR)
P1=P+H+F'(P,Z)/2.
7=Z+H/Z.
        7=7+H/7:
RJO=MMPSJC(Z1+R1,IER)
RJZ=WMPSJ1(71+R1,IER)
1 R=P+H+F7(R1,Z)
PN=P
             CALCULATE FFFICIENCY USING EQ (2-4°). FM = ETA N
```

REFERENCES

REFERENCES

- Bennett, C.O., Myers, J.E. 1962. Momentum, Heat, and Mass Transfer. McGraw-Hill.
- Berman, N.S. 1978. "Drag Reduction by Polymers." Ann. Rev. Fluid Mech. 10, 47.
- Bingham. 1922. Fluidity and Plasticity. McGraw-Hill.
- Bird, R.B., Stewart, W.E., and Lightfoot, E.W. 1960. <u>Transport</u> Phenomena. John Wiley and Sons.
- Blanks, R.F., Park, H.C., Patel, D.R., and Hawley, M.C. 1974.

 "A Rheological Study of Aqueous Separan Solutions."

 Polymer Eng. Sci. 14, 16.
- Bradley, D. and Pulling, D.J. 1959. "Flow Patterns in the Hydraulic Cyclone and Their Interpretation in Terms of Performance." Trans. Inst. Chem. Engrs., 37, 34.
- Bradley, D. 1965. <u>The Hydrocyclone</u>. Pergamon Press.
- Chiou, C.S. and Gordon, R.J. 1976. "Vortex Inhibition: Velocity Profile Measurements." AICHE Jl. 22, No. 5, 947.
- Dahlstrom, D.A. 1949. "Cyclone Operating Factors and Capacities on Coal and Refuse Slurries." Trans. Amer. Inst. Min. (Metall.) Engrs. 184, 331.
- Donohue, G.I., Tiederman, W.G., and Reischman, M.M. 1972. "Flow Visualization of the Near-Wall Region in a Drag Reducing Channel Flow." J. Fluid Mech. 56, 559, 575.
- Kelsall, D.F. 1952. "A Study of the Motion of Solid Particles in a Hydraulic Cyclone." Trans. Inst. Chem. Engrs., 30, 87.
- Kelsall, D.F. 1953. "A Further Study of the Hydraulic Cyclone." Chem. Eng. Sci., 2, 254.
- Knowles, S.R., Woods, D.R., and Feuerstein, I.A. 1973. "The Velocity Distribution Within a Hydrocyclone Operating Without an Air Core." The Canadian Jl. Chem. Eng., 51, 263.

- Metzner, A.B., Uebler, E.A., and Chan Man Fong, C.F. 1969.
 "Converging Flows of Viscoelastic Materials." AICHE
 Jl. 15, No. 5, 750.
- Mysels, K.J. 1949. "Flow of Thickened Fluids." U.S. Patent 2, 492, 173. Dec. 27, 1949.
- Nychas, S.G., Hershey, H.C., and Brodkey, R.S. 1973. "A Visual Study of Turbulent Shear Flow." J. Fluid Mech., 61, 513.
- Rietema, K. 1961. "Performance and Design of Hydrocyclones I-IV." Chem. Eng. Sci., 15, 298-325.
- _____. 1963. "Liquid-Solids Separation in a Cyclone. The Effect of Turbulence on Separation." Interaction between Fluids and Particles. (London: Inst. Chem. Engrs.), 275.
- Sylvester, N.D. and Kumor, S.M. 1973. "Degradation of Dilute Polymer Solutions in Turbulent Tube Flow." AICHE Symp. Ser., No. 130, Vol. 69, 69.
- Toms, B.A. 1948. "Some Observations on the Flow of Linear Polymer Solutions Through Straight Tubes at Large Reynolds Numbers." Proc. Ist. Int. Congr. Reol., 2, 135, 41.
- Virk, P.S. 1975. "Drag Reduction Fundamentals." AICHE Jl. 21, 625.

